2013

Effect of Exhaust Gas Recirculation and Combustible Oxygen Mass Fraction on Emission Index of NOx for Counterflow Methane/Air Diffusion Flames

Mugdha S. Sane
Purdue University

Graduate School ETD Form 9
(Revised 12/07)

PURDUE UNIVERSITY
GRADUATE SCHOOL
Thesis/Dissertation Acceptance

This is to certify that the thesis/dissertation prepared

By Mugdha S Sane

Entitled
Effect of Exhaust Gas Recirculation and Combustible Oxygen Mass Fraction on Emission Index of NOx for Counterflow Methane/Air Diffusion Flames

For the degree of Master of Science in Mechanical Engineering

Is approved by the final examining committee:

Dr. Jay P. Gore
Chair

Dr. Sameer V. Naik

Dr. Gregory M. Shaver

Dr. John Abraham

To the best of my knowledge and as understood by the student in the *Research Integrity and Copyright Disclaimer (Graduate School Form 20)*, this thesis/dissertation adheres to the provisions of Purdue University's "Policy on Integrity in Research" and the use of copyrighted material.

Approved by Major Professor(s): Dr. Jay P. Gore

Dr. Sameer V. Naik

Approved by: Dr. David Anderson 12/06/2013
Head of the Graduate Program Date

EFFECT OF EXHAUST GAS RECIRCULATION AND COMBUSTIBLE OXYGEN MASS FRACTION ON EMISSION INDEX OF NO_X FOR COUNTERFLOW METHANE/AIR DIFFUSION FLAMES

A Thesis

Submitted to the Faculty

of

Purdue University

by

Mugdha Shriram Sane

In Partial Fulfillment of the

Requirements for the Degree

of

Master of Science in Mechanical Engineering

December 2013

Purdue University

West Lafayette, Indiana

Dedicated to my parents, Dr. Suneeta Sane and Dr. Shriram Sane, my sister Medha and my brother-in-law Amogh for keeping me motivated and supporting me throughout the duration of this work.

ACKNOWLEDGEMENTS

I would like to take this opportunity to thank everyone because of whom this work has been accomplished. First and foremost I thank my major advisor Prof. Jay P. Gore for giving me the opportunity to be a part of his research group and work on this exciting topic of my interest. His constant guidance, support, insight and motivation have been the driving factors for developing this project into its current form.

I would also like to thank Dr. Sameer Naik for all his help with the computer code used for the current work. His wholehearted guidance and support during the later stages of this work are highly appreciated. I sincerely thank Dr. Shaver and Dr. Abraham for agreeing to serve on my thesis committee.

I am extremely grateful to my fellow graduate students in the research group, Indraneel Sircar and Shruthi Dasappa for helping me overcome difficulties with computer codes that I used. Thank you Neel for your help, guidance and support during this project. I appreciate all fellow students from my research group for their insightful suggestions on numerous occasions and their help.

I am greatly obliged to Cummins Inc. and School of Mechanical Engineering, Purdue University for funding my education through these two years. Finally, I would like to express my gratitude towards my family, friends and my awesome roommates, Sai and Nishi, for their constant encouragement in my every endeavor.

TABLE OF CONTENTS

Page

LIST OF TABLES

LIST OF FIGURES

Figure Page

Figure Page

Appendix Figure:

Figure Page

NOMENCLATURE

Symbols

C_p	Specific heat of gas mixture, J/kg/K
h_k	Total enthalpy of species
L	Distance between two ducts, m
P	Pressure
r	Radial co-ordinate, m
T	Temperature
u	Axial velocity, m/s
v	Radial velocity, m/s
x	Axial co-ordinate, m
X_k	Mole fraction of species k
Y_k	Mass fraction of species k
Z	Mixture fraction

Greek Symbols

ρ	Density of gas mixture, kg/m^3
λ	Thermal conductivity of gas mixture

Subscripts

F	Fuel stream
O	Oxidizer stream
AIR	Oxidizer stream
FUEL	Fuel stream
Pr	Products
Ox	Oxidizer

ABSTRACT

Sane, Mugdha, M.S., Purdue University, December 2013. A Study on the Effect of Exhaust Gas Recirculation and Combustible Oxygen Mass Fraction on Emission Index of NO_x for Counterflow Diffusion Flames. Major Professors: Dr. Jay P. Gore And Dr. Sameer V. Naik, School of Mechanical Engineering.

Exhaust gas recirculation has been proven to be an effective method of reducing emissions of oxides of nitrogen (NO_x) from internal combustion engines. The present study validates this effect through flame simulations using detailed chemistry. Counterflow methane/air diffusion flames were simulated in one dimension in physical space using GRI-Mech 3.0 detailed chemistry mechanism, thermal, and transport data. The influence of Exhaust Gas Recirculation (EGR) on the flame structure and NO_x emissions was studied by selecting higher than ambient inlet temperature and by varying the composition of the oxidizer stream. The Combustible Oxygen Mass Fraction (COMF), which represents the fraction of total inlet oxygen available for combustion, was varied by selecting EGR fractions between 5% and 40%.

The results showed that the emission index of NO_x ($EINO_x$) is directly proportional to the COMF in agreement with recent experimental observations from engine studies. The $EINO_x$ computations also captured experimentally observed decrease in the pressure exponent reported in recent experimental studies. In addition to pressure and preheat, the effect of variation in strain rate on the flame structure and NO_x emissions

is also studied. Similar to low strain rate flames without EGR, low strain rate flames with EGR are also observed to have higher NO_x emissions.

A linear relation between COMF and stoichiometric fuel/air ratio has been observed. The application of detailed chemistry calculations to develop $EINO_x$-COMF control algorithms is promising.

CHAPTER 1. INTRODUCTION

1.1 Background

Internal combustion engines are the primary means of powering commercial land, rail, and marine transportation in the world. Their fuel efficiency, durability and reliability make them an attractive prime mover. According to a survey (Schneider and Hill, 2005), there were about 13 million diesel engines in the USA in 2005, and the number is increasing continuously. While the engines are efficient and reliable, many challenges still remain to be addressed.

The primary challenge with diesel engines is related to emissions. NO_x, which is a major effluent from engines, results in respiratory infections (Kampa & Castanas 2008), acid rains, and reduction in oxygen carrying capacity of blood (Paul et al. 2008). To address these concerns, the US Environmental Protection Agency (EPA) has imposed strict regulations on the exhaust emissions of diesel engines. Table 1.1 shows the evolving NO_x standards over the years for new trucks and buses (US Environmental Protection Agency). The EPA emission standards are based on the amount of pollutant emitted per unit energy produced at the wheels, expressed in grams per brake horse power hour (g/bhp-hr) or grams per kilowatt hour (g/kW-hr).

Table 1-1 EPA Emissions for new trucks and buses for PM and NOx from 1984 to 2010 (g/bhp-hr).

Year	Nitrogen Oxide (NOx)
1984	10.7
1991	5
1994	5
1998	4
2004	2
2007-2010	0.2

It can be observed from Table 1.1 that the regulatory limits on the pollutants have become increasingly stringent over the years. Researchers all over the world are involved in developing new technologies to meet these regulations. Several technologies have been proposed and implemented to reduce emissions either through in-cylinder combustion modifications or by employing after-treatment devices.

Most after-treatment devices used for NO_x reduction are associated with a penalty in fuel consumption and design modifications (Heywood 1988). Exhaust gas recirculation is an effective technique of reducing NO_x emissions substantially (Heywood 1988; Turns 2010). Partial recirculation of exhaust gas, in combination with other techniques, has recently become essential, for attaining lower emission levels. Nitric oxide (NO) is formed inside the combustion chamber in post-flame combustion process in the high temperature region by various mechanisms. The NO formation and decomposition inside the combustion chamber can be mainly described by the Zeldovich (thermal NO) mechanism (Turns 2010). NO formation by thermal mechanism is related to the rate coefficient, oxygen and nitrogen concentration and temperature. The NO formation

reaction is highly sensitive to temperature and oxygen concentration as observed by studying NO_x formation at 1800 K (Plee et al. 1982). Hence, in order to reduce NO_x formation during the combustion process, the temperature and oxygen concentration in the combustion chamber need to be reduced.

Literature suggests that adding EGR to the incoming air flow in a Diesel engine, rather than displacing some of the inlet air, appears to be a more beneficial way of utilizing EGR in Diesel engines (Abd-Alla 2002). This method may allow exhaust NO_x emissions to be reduced substantially. However, EGR also reduces the combustion rate, which may make stable combustion more difficult to achieve. The brake specific fuel consumption decreases with increasing EGR with constant burn duration and brake mean effective pressure. The improvement in fuel consumption with increasing EGR is due to three factors: (1) reduced pumping work, (2) reduced heat loss to the cylinder walls, and (3) a reduction in the degree of dissociation in the high temperature burned gases. In dual fuel engines (with Diesel and natural gas) using hot EGR, the thermal efficiency improves due to increased intake charge temperatures and reburning of the unburned fuel in the recirculated gases. Simultaneously, NO_x and smoke is reduced to almost zero at high natural gas fractions. Cooled EGR gives lower thermal efficiency compared to hot EGR, but lower NO_x emissions are possible.

1.2 Exhaust Gas Recirculation Theory

The exhaust gases mainly consist of carbon dioxide, nitrogen, and water vapor, all of which have higher specific heats compared to atmospheric air. This leads to a reduction in the flame temperature, consequently affecting NOx production. Recirculated

exhaust gas displaces fresh air entering the combustion chamber with carbon dioxide and water vapor. Consequently lower amount of oxygen in the intake mixture is available for combustion (Abd-Alla 2002; Agarwal et al. 2011)

The sudden interest in EGR technology as a method of lowering NO_x emissions can be attributed to several reasons (Chandler et al. 2012). Firstly, newer environmental regulations pose tighter challenges for reducing NO_x emissions as seen from Table 1.1. Secondly, further reductions in NO_x emissions have probably become the most difficult target to attain owing to undesired effects of techniques such as high supercharging. Thirdly, the development of a new generation of EGR valves and improvements in electronic controls allow a better EGR accuracy and shorter response time in transient conditions. Finally, the inclusion of particulate emission regulations in the early 1990s, which are more stringent than those of smoke capacity, has redirected efforts to reduce emissions in terms of mass, rather than in terms of concentration, which can be favored by reducing the total exhaust mass flow rate.

Studies on Diesel engines with exhaust gas recirculation (Adi et al. 2009; Adi 2012) have shown that increasing exhaust gas recirculation reduces NO_x emissions. The Emission Index of NO_x ($EINO_x$) is inversely proportional to the Combustible Oxygen Mass Fraction (COMF) (Adi et al. 2009), which represents the total fraction of oxygen in the reacting species, contributed by fresh air, EGR and fuel.

A six cylinder, turbocharged, cooled EGR Diesel engine was used in the experiments by Adi et al. Fig. 1-1 shows a schematic of the engine. A fraction of exhaust gases from the engine is directed towards the EGR cooler and the remaining goes to

turbine inlet. Addition of EGR increases the boost pressure due to the extra mass now entering the cylinder.

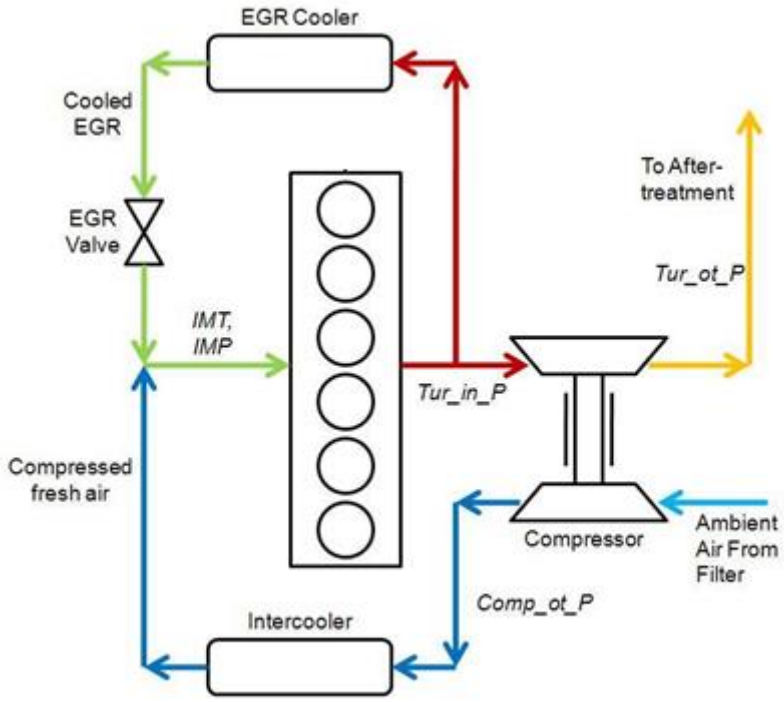

Figure 1-1 Engine Schematic.

Figure 1-2 is a schematic illustrating the correspondence between a flame created in a Diesel engine cylinder at the end of every compression stroke, and it's approximation as a laminar counterflow diffusion flame. The oxidizer stream entering the combustion chamber contains EGR, in addition to fresh air. Out of the numerous flamelets inside the combustion chamber, a single flamelet is simulated in the present study. The Diesel flame is approximated by a counterflow methane air diffusion flame. The oxidizer stream consists of O_2 and N_2 from fresh air and CO_2 and H_2O added through EGR.

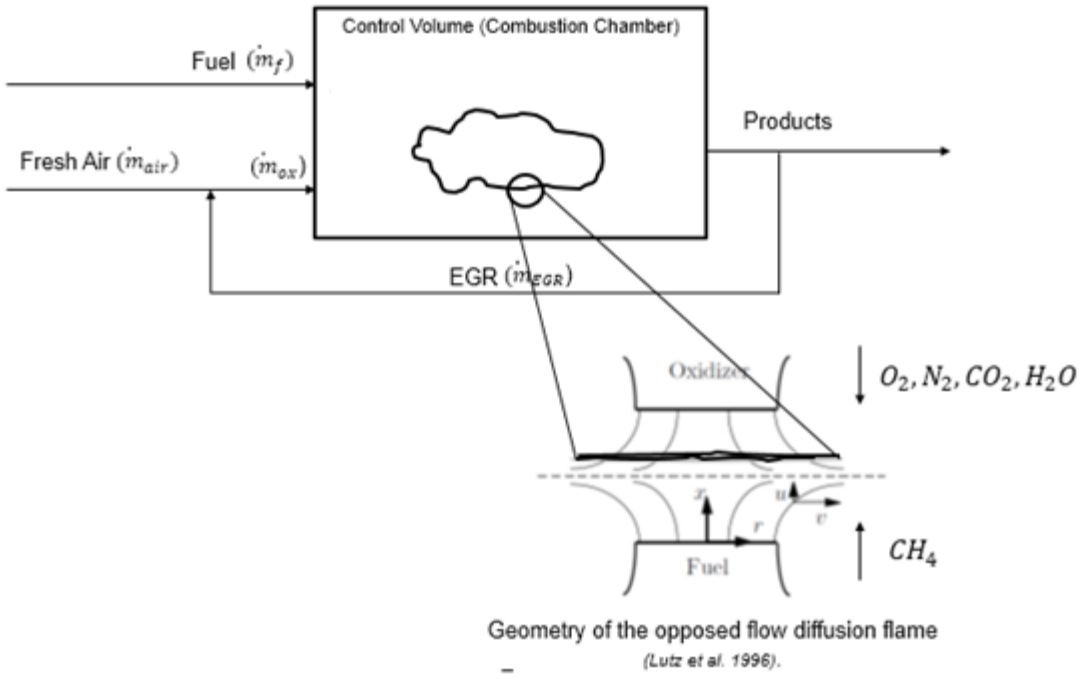

Figure 1-2 Combustion chamber and flame schematic.

The composition of fuel and oxidizer streams can be defined be a function of a conserved scalar called mixture fraction. It is defined as

$$Z = \frac{Mass\ of\ material\ having\ its\ origin\ in\ the\ fuel\ stream}{Mass\ of\ mixture}. \quad (1)$$

In terms of oxidizer-fuel ratio (ν), mixture fraction can be represented as

$$Z = Y_F + \left(\frac{1}{\nu+1}\right) Y_{Pr}\ . \quad (2)$$

The oxidizer composition for x % EGR is given by

$$(1 - 0.01x) \times \frac{2}{\emptyset}(O_2 + 3.76N_2) + 0.01x\left(CO_2 + 2H_2O + \frac{7.52}{\emptyset}N_2 + \frac{2(1-\emptyset)}{\emptyset}O_2\right). \quad (3)$$

The objective of this study is to analyze the effect of exhaust gas recirculation on NO_x emissions through counterflow diffusion flame simulations using the GRI-Mech 3.0 (Smith et al.) detailed chemistry mechanism.

Previous flame studies (Blevins 1996) have discussed the structure of counterflow diffusion flames through burner experiments and simulations using the OPPDIF(Lutz et al. 1996) code.

In the present study of the effect of air preheat on flame structure of counterflow methane-air diffusion flames, a 50% increase in the peak NO mole fraction was observed with increase in inlet air temperature from 300 K to 500 K. The increase in peak NO mole fractions with air preheat occurs primarily through enhanced reaction rate of the prompt initiation reaction. The NO production by the thermal mechanism increases significantly with air preheat, but still remains a very small portion of the total (Lim, Gore, & Viskanta, 2000).

At high pressures, NO_x emissions shoot up significantly(Chadwick et al. 2001; Figura & Gomez 2012; Briones et al. 2007). In this study, it has been observed that the effect of pressure on NO_x emissions is nearly as significant as its effect on heat release rate. Hence at high pressures, the emission index of NO_x, which is normalized by heat release, shows less sensitivity to pressure.

In addition to temperature and pressure, strain rate and radiation also affect NO_x emissions significantly. The effect of radiation on temperature becomes more pronounced as strain rate decreases (Zhu & Gore 2005). These effects are mirrored in the dependence of peak nitric oxide concentration on strain rate – at lower strain rates, more nitric oxide is produced in the flame (Vranos & Hall 1993). Moreover, neglecting radiation heat loss leads to significantly higher estimates of NO compared to estimates including radiation heat loss, particularly at high pressures (Zhu & Gore 2005). In the present study, the effect of radiation has been considered.

Although the exact value of the emission index of NO_x varies with the fuel, the $EINO_x$– COMF relationship is consistent irrespective of the fuel used. Typically, n-heptane is considered to be a suitable surrogate for gasoline and dodecane often substitutes Diesel for the purposes of study. It is observed that heptane-air flames have higher $EINO_x$ than methane-air diffusion flames. The amounts of C_2H_2 and CH radicals formed in n-heptane flames are significantly higher than those in methane flames and are responsible for the observed differences in NO_x characteristics of the two fuels (Naha and Aggarwal 2004).These radicals are primarily important in the prompt NO chemistry. This is indicative of the importance of prompt NO mechanism over thermal NO mechanism, as studied previously (Lim et al. 2000). The present study shows that in spite of quantitative differences in $EINO_x$, the qualitative behavior of decrease in $EINO_x$ with EGR addition is similar to that observed through engine experiments.

1.3 Objectives of the present work

The objective of the current study is to study the effect of exhaust gas recirculation on premixed, partially premixed, and diffusion flame NO_x emissions. The aim is to emulate the $EINO_x$ – COMF relationship for flames combusting real oxygenated fuel using the numerical code OPPDIF, employing detailed chemistry, to show that the simplified models with gaseous methane fuel qualitatively captures the effect of EGR leading to lower NO_x emissions, that has been validated for Diesel engines through experiments (Adi et al. 2009).

It has been previously established that engine flames have non-premixed, premixed, and partially premixed configurations. The present thesis focuses on the non-

premixed flame configuration. Preliminary studies of premixed flames with EGR were also completed and are presented in Appendix A.

The study also focuses on the effect of global strain rate on methane-air combustion. GRI-Mech 3.0 detailed chemistry is employed for all flame calculations.

Table 1-2 Input variables and their parametric range for current study.

Input variable	Parametric range
Global strain rate	20 to 40 s^{-1}
Thermal diffusion	On
Radiation	On
Pressure	1, 5, 10, 20 bar
Preheat	300 and 500 K
EGR fraction	0,5,10,15,20,40%

The present study clarifies the relationship between Combustible Oxygen Mass Fraction (COMF), Air/fuel rat io and EGR fraction.

1.4 Outline

Chapter 2: COMPUTATIONAL MODEL explains the computational domain, assumptions, and governing equations employed for the detailed chemistry calculations. An introduction to calculation of other variables used through the thesis is presented.

Chapter 3: EFFECTS OF EXHAUST GAS RECIRCULATION ON COUNTERFLOW METHANE/AIR DIFFUSION FLAMES presents the results from flame calculations using OPPDIF and detailed chemistry. The effect of variation of EGR, pressure, preheat,

and strain rate on the flame structure and emissions of counterflow diffusion flames is presented. This chapter also includes the comparison between the calculations of the present work and previous experimental results for counterflow methane-air diffusion flames.

Chapter 4: SUMMARY, CONCLUSIONS AND RECOMMENDATIONS FOR FUTURE WORK outlines the key findings of this work and suggestions for expanding the current study.

APPENDIX A includes results from simulations of premixed methane air flames to study the effect of EGR variation, preheat, and pressure on NOx emissions.

CHAPTER 2. THEORETICAL AND COMPUTATIONAL MODEL

Opposed flow diffusion flames is a configuration representing laminar flames in many practical environments as per the theory proposed by Williams and Peters(Peters & Williams 1983).Calculations of opposed flow flames with detailed chemistry, including NO_x chemistry, have been conducted since long time. The laminar flamelet theory relies on an experimental observation by Bilger (Bilger 1988) stating that all stable species can be expressed as a function of a conserved scalar i.e. mixture fraction. Modeling and computations of laminar flamelet (Sivathanu & Faeth 1990; Bilger 2006; Berta et al. 2006) and experimental verifications of the laminar flamelet concept have been provided (Blevins & Gore 1999; Blevins et al. 1999; Lim et al. 2000).The purpose of this work is to utilize laminar flamelet calculations to study NO_x emissions from non-premixed flames with and without preheat at atmospheric and high pressures with specific emphasis on inlet oxygen concentrations as typically employed in the Exhaust Gas Recirculation (EGR) strategy. More specifically, recent experimental observations(Adi et al. 2009; Adi 2012)for biofuel combustion in Diesel engine have shown that NO_x emissions expressed in the form of $EINO_x$ not only decrease significantly with EGR but their values are also correlated with a quantity defined as Combustible Oxygen Mass Fraction (COMF).

The laminar flamelet calculations were done using OPPDIF code (Lutz et al. 1996) OPPDIF is a Fortran program that computes the diffusion flame between two opposing nozzles. A similarity transformation reduces the two-dimensional axisymmetric flow problem to a one-dimensional problem. Assuming that the radial component of velocity is linear in radius, the dependent variables become functions of the axial direction only. OPPDIF solves for the temperature, species mass fractions, axial, and radial velocity components as well as radial pressure gradient, as an Eigen value problem. The Two Point software solves the two-point boundary value problem for the steady state form of the discretized equations. The Chemkin package evaluates chemical reaction rates and thermodynamic and transport properties

2.1 Computational Domain for the Counterflow Configuration

The geometry consists of two concentric, circular nozzles directed towards each other, as shown in Fig. 2.1.

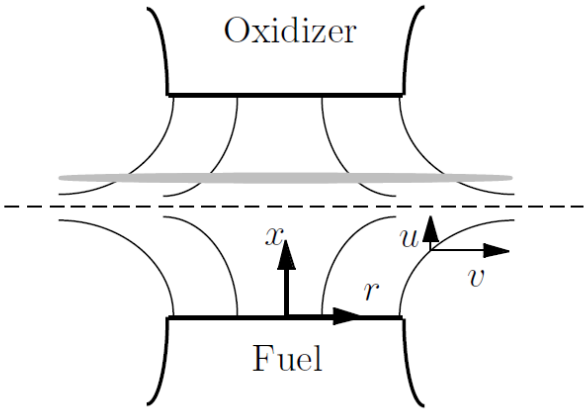

Figure 2-1 Geometry of the opposed flow diffusion flame (Lutz et al. 1996).

This configuration produces an axisymmetric flow with a stagnation plane between the nozzles. The location of the stagnation plane depends on the momentum balance of the two streams. When the streams are premixed, two premixed flames exist, one on either side of the stagnation plane. When one stream contains fuel, and the other oxidizer, a diffusion flame is established. Since most fuels require more air than fuel by mass, the diffusion flame usually sits on the oxidizer side of the stagnation plane; fuel diffuses through the stagnation plane to establish the flame in a stoichiometric mixture.

The opposed flow geometry makes an attractive experimental configuration, since the flames are flat, allowing for comprehensive study of the flame structure using detailed chemistry.

The reduction of the two dimensional stagnation flow is based upon similarity solutions advanced for incompressible flows by von Karman, which are more easily available in Schlichting (Schlichting 1968). Numerical solutions for diffusion flames in this geometry were produced by Hahn et al.(Hahn & Wendt 1981) Solutions on the similar geometry of a counterflow stagnating on a porous cylinder, originally studied by Tsuji(Tsuji & Yamaoka 1967), were advanced during the GAMM workshop(Dixon-Lewis et al. 1985).

GRI-Mech 3.0 detailed chemistry was employed for the calculations. GRI-Mech 3.0(Smith et al.) is an optimized mechanism designed to model natural gas combustion, including NO formation. It is a compilation of 325 elementary chemical reactions and associated rate coefficient expressions and thermochemical parameters for the 53 species involved in them.

2.2 Governing Equations for the Laminar Counterflow Flame

At steady state, conservation of mass in cylindrical co-ordinates is

$$\frac{\partial}{\partial x}(\rho u) + \frac{1}{r}\frac{\partial}{\partial r}(\rho v r) = 0. \tag{4}$$

where u and v are the axial and radial velocity components and ρ is the mass density. Following von Karman, who recognized that v/r and other variables should be functions of x only, which gives

$$G(x) = -\frac{\rho v}{r}. \tag{5}$$

$$F(x) = \frac{\rho u}{2}. \tag{6}$$

For which continuity reduces to

$$G(x) = \frac{dF(x)}{dx}.$$

$$H = \frac{1}{r}\frac{\partial p}{\partial r} = constant.$$

Radial momentum equation is given by

$$H - 2\frac{d}{dx}\left(\frac{FG}{\rho}\right) + \frac{3G^2}{\rho} + \frac{d}{dx}\left[\mu\frac{d}{dx}\left(\frac{G}{\rho}\right)\right] = 0. \tag{7}$$

Energy and species conservation is given by

$$\rho u\frac{dT}{dx} - \frac{1}{c_p}\frac{d}{dx}\left(\lambda\frac{dT}{dx}\right) + \frac{\rho}{c_p}\sum_k c_{p_k} Y_k V_k \frac{dT}{dx} + \frac{1}{c_p}\sum_k h_k \dot{\omega}_k = 0. \tag{8}$$

$$\rho u\frac{dY_k}{dx} + \frac{d}{dx}(\rho Y_k V_k) - \dot{\omega}_k W_k = 0; k = 1, \tag{9}$$

The boundary conditions for the fuel (F) and oxidizer (O) streams at the nozzle are

$$x = 0: F = \frac{\rho_F u_F}{2}, G = 0, T = T_F, \rho u Y_k + \rho Y_k V_k = (\rho u Y_k)_F. \tag{10}$$

$$x = L: F = \frac{\rho_O u_O}{2}, G = 0, T = T_O, \rho u Y_k + \rho Y_k V_k = (\rho u Y_k)_O. \quad (11)$$

The inflow boundary condition specifies the total mass flux, including diffusion and convection, rather than the species fraction$\left(Y_k = Y_{k,F}\right)$. If gradients exist at the boundary, these conditions allow diffusion into the nozzle.

The differential equations (5) through (11) form a boundary value problem for the dependent variables(F, G, H, T, Y_k). The Chemkin (Kee et al. 1996) library of subroutines provides the reaction rates and thermodynamic properties. A Chemkin based package evaluates the transport properties.

Strain rate is defined as the normal gradient of the normal component of the flow velocity, and changes from the fuel duct exit to oxidizer duct exit (Seshadri 2005). The global strain rate is defined as

$$a = \frac{|u_{fuel}|+|u_{ox}|}{L}. \quad (12)$$

2.3 Laminar Flamelet Calculations of $EINO_x$

The laminar flamelet approximation involves specification of species concentration as a function of a conserved scalar such as mixture fraction and scalar dissipation rate (Chen et al. 1993; Rotexo Copyright Document 2010). These functions are called state relationships and have been determined from experimental data for various fuels(Sivathanu & Faeth 1990; Gore & Skinner 1991). The state relationships can also be obtained from detailed chemistry calculations and comparison between the results of such calculations with experimental data are important. One of the hypotheses of the work

reported here is that the state relationships apply for methane/air combustion with air with and without exhaust gas recirculation.

To compute $EINO_x$ for flames studied in the physical space, the following relation developed by Blevins et al. (Blevins 1996)was used, as given by

$$EINO_x = \frac{-2\int_0^L G(x)\left(X_{NO}+X_{NO_2}\right)\frac{MW_{NO_2}}{MW_{mix}}dx}{2F_{x=0}X_{F,x=0}\left(\frac{MW_{F,x=0}}{MW_{mix,x=0}}\right)+2\int_0^L G(x)X_F\frac{MW_F}{MW_{mix}}dx}. \quad (13)$$

2.4 Exhaust Gas Recirculation and Computation of Combustible Oxygen Mass Fraction (COMF)

The composition of EGR (and hence, oxidizer composition) was determined considering complete combustion of methane, given by

$$CH_4 + \frac{2}{\emptyset}(O_2 + 3.76N_2) \rightarrow CO_2 + 2H_2O + \frac{7.52}{\emptyset}N_2 + \frac{2(1-\emptyset)}{\emptyset}O_2. \quad (14)$$

The oxidizer composition with *x*% EGR would be

$$(1 - 0.01x) \times \frac{2}{\emptyset}(O_2 + 3.76N_2) + 0.01x\left(CO_2 + 2H_2O + \frac{7.52}{\emptyset}N_2 + \frac{2(1-\emptyset)}{\emptyset}O_2\right). \quad (15)$$

The Combustible Oxygen Mass Fraction (COMF) has been defined for engine experiments by the following relationship (Adi, 2012) as

$$COMF = \frac{Y_{O_2,fuel}\dot{m}_{fuel}+Y_{O_{2,air}}\dot{m}_{air}+Y_{O_{2,EGR}}\dot{m}_{EGR}}{\dot{m}_{fuel}+\dot{m}_{air}+\dot{m}_{EGR}} = \frac{Y_{O_2,fuel}\dot{m}_{fuel}+Y_{O_{2,ox}}\dot{m}_{ox}}{\dot{m}_{fuel}+\dot{m}_{ox}}. \quad (16)$$

To calculate COMF for the simulated opposed flow diffusion flames studied here, $\dot{m}_{fuel}$, $\dot{m}_{ox}$ and $\dot{m}_{EGR}$ have been replaced by molecular weights of fuel, air and EGR respectively.

COMF represents the fraction of total oxygen in the cylinder that is available for combustion. The total oxygen includes oxygen from the charge (i.e. fresh air and recirculated exhaust gases) and the fuel (in case of oxygenated fuel).For calculating the oxygen fraction from exhaust gases, it is assumed that exhaust gas is composed of only CO_2, H_2O, and N_2. Minor product species are excluded.

CHAPTER 3. EFFECTS OF EXHAUST GAS RECIRCULATION ON COUNTERFLOW METHANE/AIR DIFFUSION FLAMES

The effect of variation in the amount of EGR added to the oxidizer flow, pressure, preheat, and strain rate was studied by simulating counterflow methane-air diffusion flames. The aim was to understand the flame structure and emissions of NO and NO_2 from the flames affected by these factors. In this chapter, effects of all these parameters are analyzed in detail.

3.1 Comparison of Computational Results with Experimental Data

For the purpose of comparison of the computational results with those from experiments, the counterflow methane-air diffusion flame was also simulated in physical space using OPPDIF. The effects of air preheat (300 to 560 K) on the flame structure of counterflow methane-air diffusion flames, was previously studied by Lim et al. (1998). Species concentrations for H_2, N_2, O_2, CH_4, CO, CO_2, C_2H_2, and C_2H_4 were measured by Lim et al. using sampling and gas chromatography. Concentrations of NO were measured using sampling and chemiluminescence analysis. Computational results for flame structure, derived from the present study are compared with these experimental results. The water component in the sample gas was condensed before entering the sampling bulb using a coiled condenser. The experimental data is thus, dry based. However, the

computational results do consider water vapor species. Mixture fraction space is used as the X-axis for the purpose of being consistent with previous data from experiments.

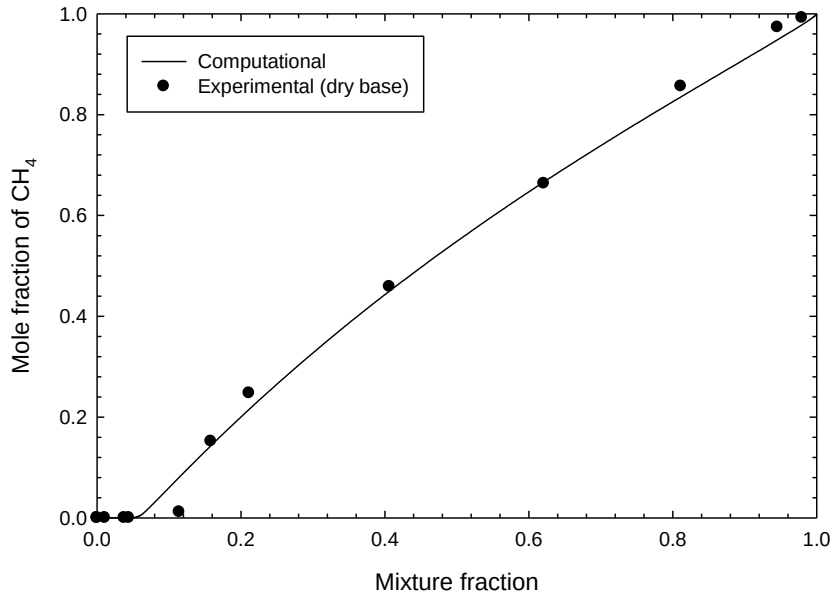

Figure 3-1 Comparison of experimental and computational data for mole fraction of CH_4.

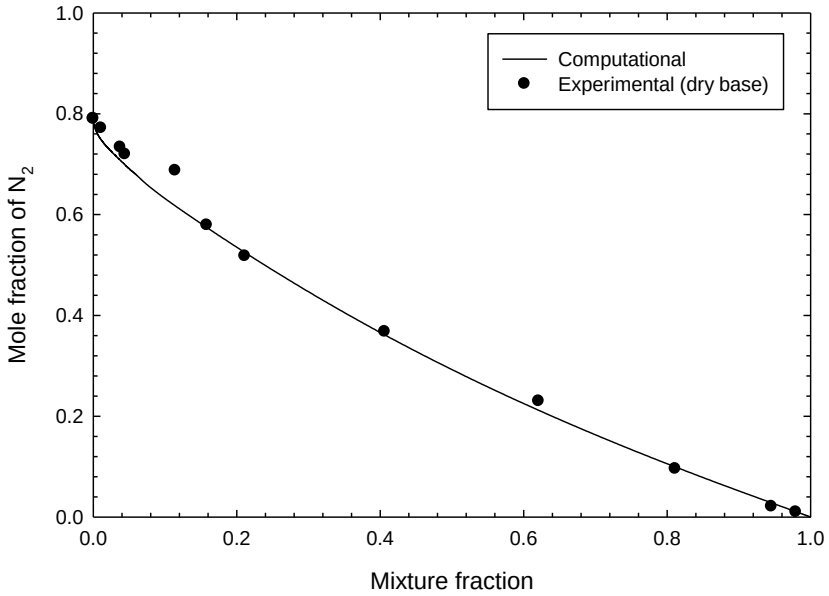

Figure 3-2 Comparison of experimental and computational data for mole fraction of N_2.

Figures 3-1 and 3-2 show mole fractions of CH_4 and N_2 plotted against mixture fraction. The computational and experimental data show fair amount of agreement throughout the range of mixture fractions.

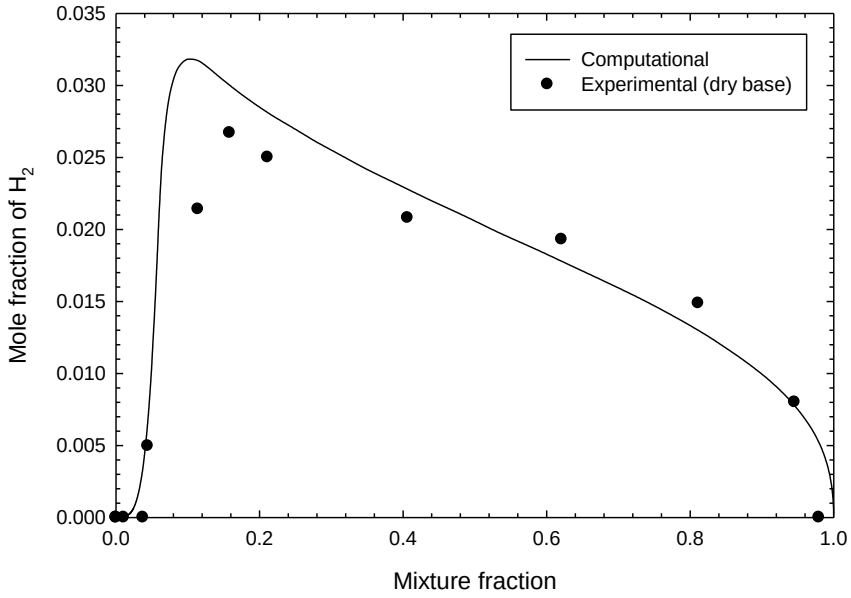

Figure 3-3 Comparison of experimental and computational data for mole fraction of H_2.

Figure 3-3 shows mole fraction of H_2 plotted against mixture fraction. It is seen that the OPPDIF results underpredict the species mole fraction in the stoichiometric to rich mixture fraction region. Perhaps, non-intrusive laser-based measurements could be used in place of gas chromatography to reduce these discrepancies.

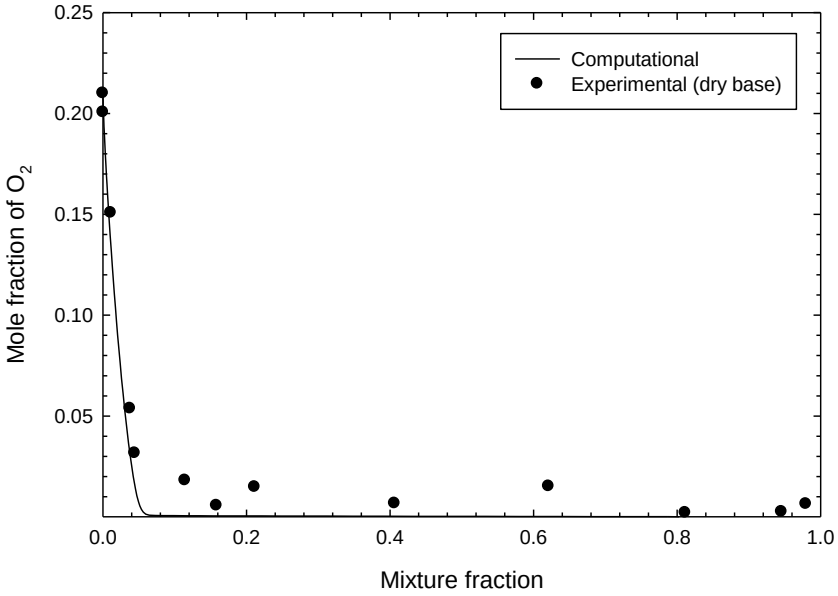

Figure 3-4 Comparison of experimental and computational data for mole fraction of O_2.

Figure 3-4 shows a comparison between measured and computed mole fractions of O_2 at different values of mixture fraction. The O_2 mole fraction drops from 0.21 at zero mixture fraction to 0.01 at mixture fraction equal to 0.1. The computational and experimental data show good agreement on the oxidizer side.

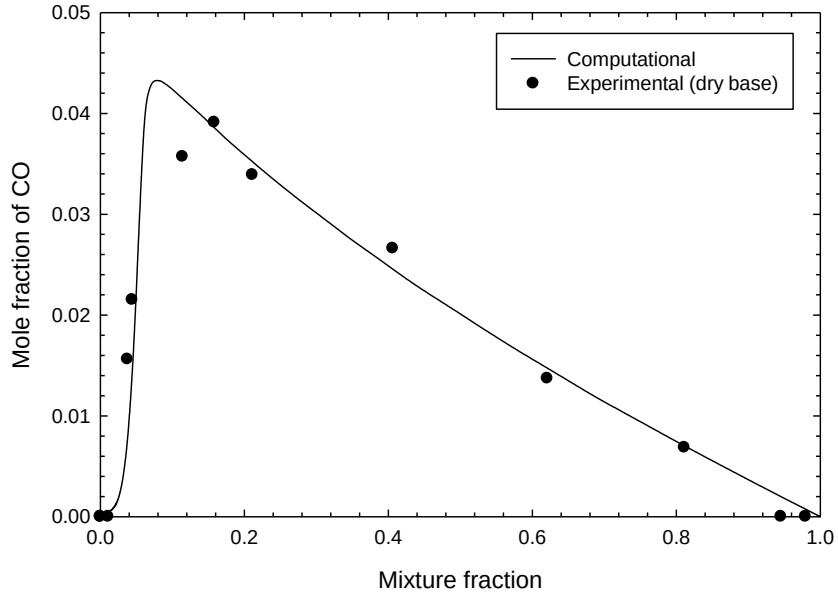

Figure 3-5 Comparison of experimental and computational data for mole fraction of CO.

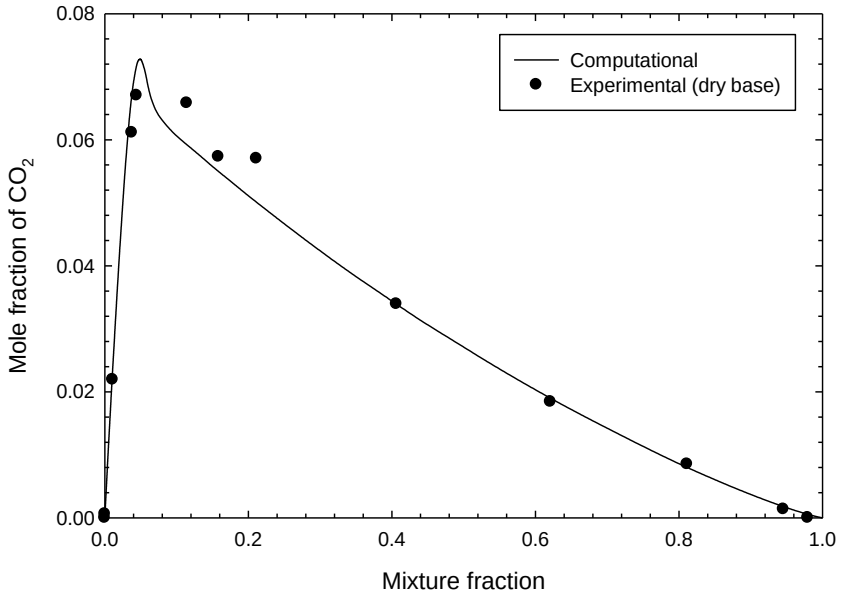

Figure 3-6 Comparison of experimental and computational data for mole fraction of CO_2.

Figures 3-5 and 3-6 show comparison of experimental and computational data for mole fractions of CO and CO_2 against mixture fraction. The experimental and computational data show fair agreement in both cases. The values of calculated mole fractions of CO, CO2, H2 and H2O were also checked using the water-gas shift equilibrium reaction given by

$$CO + H_2O \leftrightarrow CO_2 + H_2. \tag{17}$$

The equilibrium constant for the above reaction is given by

$$K_P = \frac{(P_{CO_2}/P^0)\cdot(P_{H_2}/P^0)}{(P_{CO}/P^0)\cdot(P_{H_2O}/P^0)}. \tag{18}$$

The equilibrium constant at 1970 K was calculated to be 0.2.

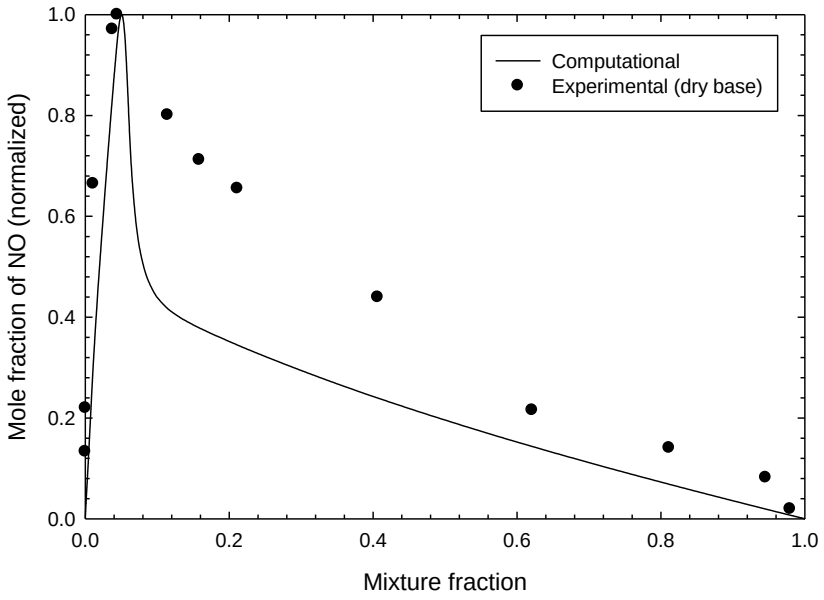

Figure 3-7 Comparison of experimental and computational data for mole fraction of NO.

Figure 3-7 shows variation in NO mole fraction with mixture fraction, for computed and experimental data. Discrepancy is observed between measurements and computational results on the fuel-rich side where the measured NO profile is much wider than that in

computational results. In this region, the computed values are almost 40% lower than measurements. This is one of the well-known deficiencies in modeling of the prompt NOx mechanism in GRI-Mech 3.0.

3.2 Effect of Variation in the Exhaust Gas Fraction

Six different operating conditions listed in Table 3-1 were chosen to analyze the effect of exhaust gas recirculation on the structure and NO_x emissions of counterflow methane-air diffusion flames. EGR fraction was changed while maintaining inlet air and fuel temperature, strain rate, and pressure. The effect of addition of EGR leading to an increase in pressure inside the cylinder of a Diesel engine is not considered here. It is assumed that pressure is 1 bar for all cases, irrespective of EGR fraction.

Table 3-1 Operating conditions for analyzing the effect of EGR on flame structure and EINOx.

Case	Pressure (Bar)	Oxidizer/Fuel Inlet Temperature (K)	EGR Fraction (%)
1	1	300	0
2	1	300	5
3	1	300	10
4	1	300	15
5	1	300	20
6	1	300	25

For simulating the counterflow flames in OPPDIF, the following input mole fractions listed in Table 3-2 were used:

Table 3-2Moles of reacting species at different EGR fractions.

% EGR	Moles of CH_4	Moles of O_2	Moles of N_2	Moles of CO_2	Moles of H_2O
0	1	2	7.52	0	0
5	1	1.9	7.52	0.05	0.1
10	1	1.8	7.52	0.1	0.2
15	1	1.7	7.52	0.15	0.3
20	1	1.6	7.52	0.2	0.4
25	1	1.5	7.52	0.25	0.5

A separation distance of 2 cm between the fuel (methane) and air ducts was specified. A flow velocity of 30 cm/s was specified for both streams. Thus, the computed flame had a constant global strain rate of 30 s^{-1}. Fuel and oxidizer inlet temperature was specified to be 300 K.

Referring to equation (9), X_{NO} and X_{NO_2} are obtained directly from OPPDIF results. G(x) and F are calculated using equations (2) and (3). The calculation of COMF does not depend on results from computations, since it requires only fuel and oxidizer composition. By knowing % EGR, composition of oxidizer is derived using eq. (11). This is then used in equation (12) for calculating COMF. Values of $EINO_x$ and COMF for different EGR fractions are shown in Table 3-3.

Table 3-3EINOx and COMF for different EGR fractions.

EGR Fraction (%)	COMF	EINOx (g/hP-hr)
0	0.21	3.34
5	0.21	2.89
10	0.20	2.24
15	0.18	1.55
20	0.17	0.76
25	0.16	0.43
40	0.14	3.78e-8

The computed wet based mole fraction results presented below. The following figures are plotted with respect to axial coordinate to facilitate better understanding of the flame stabilization location and overall structure.

Figure 3-8 represents the temperature profile plotted against distance from the fuel nozzle exit for different EGR fractions. It is seen that with increasing amount of EGR in the oxidizer stream, peak flame temperatures are lowered. The flame also shifts slightly towards the oxidizer side to compensate for lowered amount of oxygen available in the oxidizer. The temperature profile becomes narrower with increase in the EGR fraction in the oxidizer. This is in accordance with the theory of heat absorption by species present in exhaust gases leading to lower peak flame temperatures.

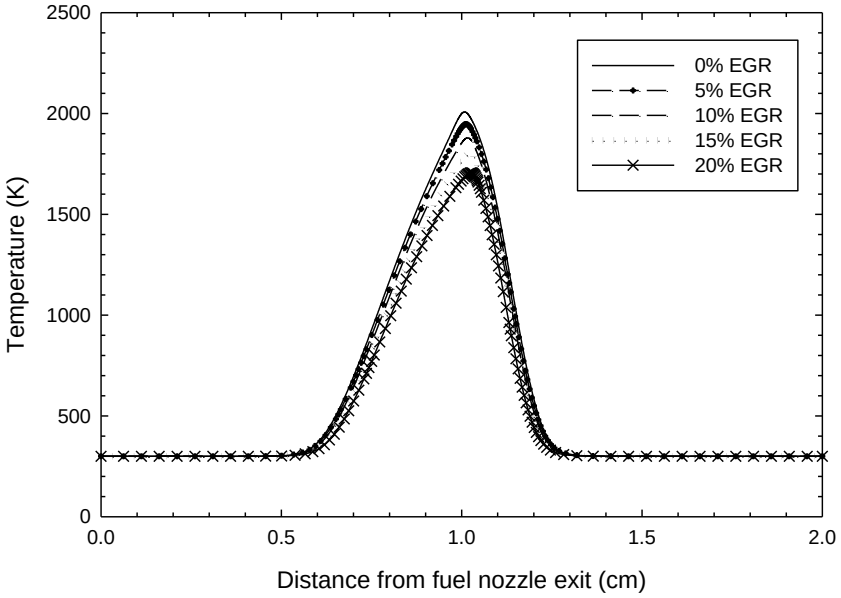

Figure 3-8 Temperature vs. axial co-ordinate for different amounts of EGR.

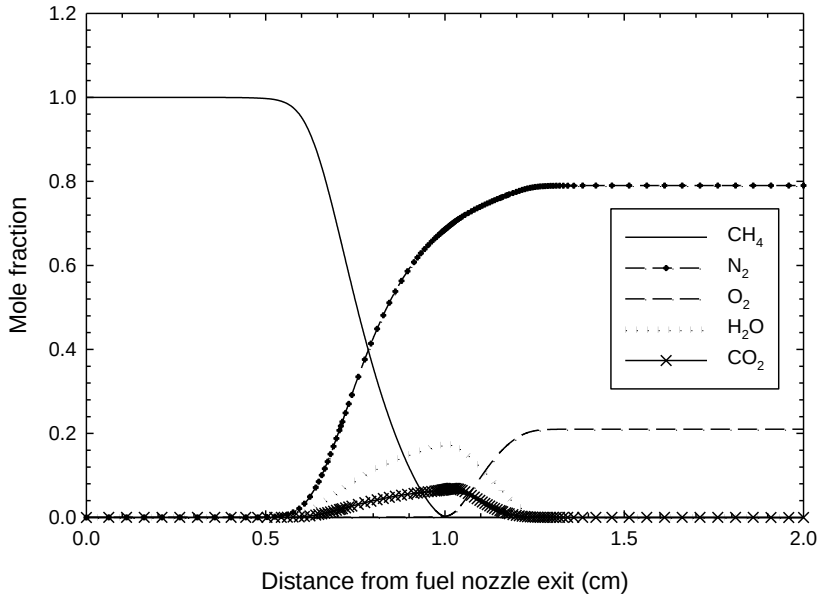

Figure 3-9 Major species' mole fractions vs. axial co-ordinate for 0% EGR.

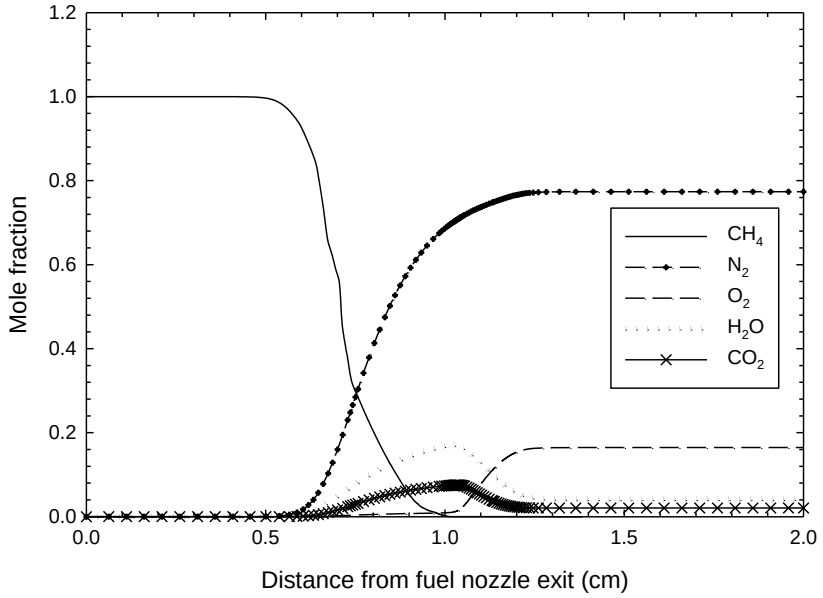

Figure 3-10 Major species' mole fractions vs. axial co-ordinate for 20% EGR.

Figures 3-9 and 3-10 show the major species mole fractions plotted against distance from the fuel exit for 0% and 10% EGR fraction. Minor changes in flame structure are observed. The flame seems to stabilize slightly towards the oxidizer side for the higher EGR case.

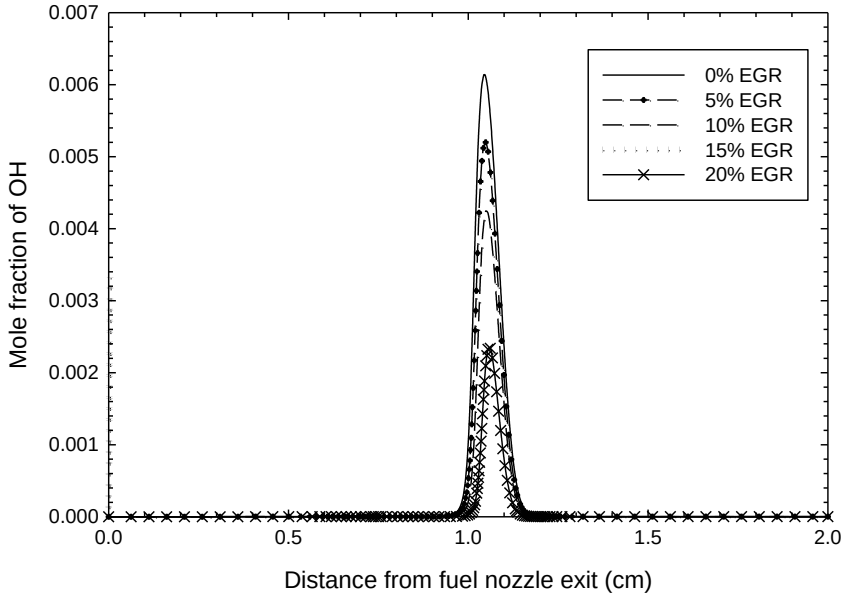

Figure 3-11 Mole fraction of OH vs. axial co-ordinate for different amounts of EGR.

Figure 3-11 shows the OH mole fraction plotted against distance from the fuel exit. The peak OH mole fraction moves towards the oxidizer side with increasing addition of exhaust gases to the reacting mixture. The location of the peak OH mole fraction seems to be independent of the EGR fraction.

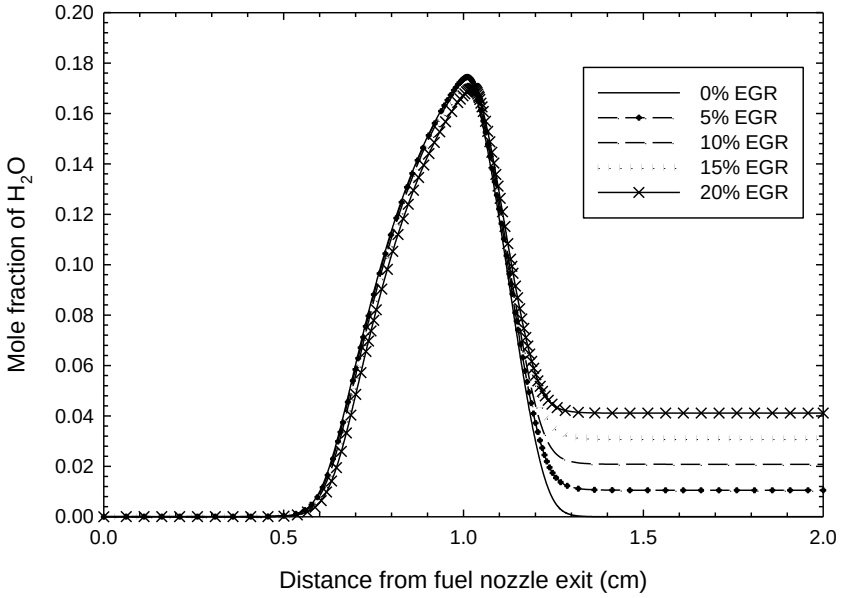

Figure 3-12 Mole fraction of H_2O vs. axial co-ordinate for different amounts of EGR.

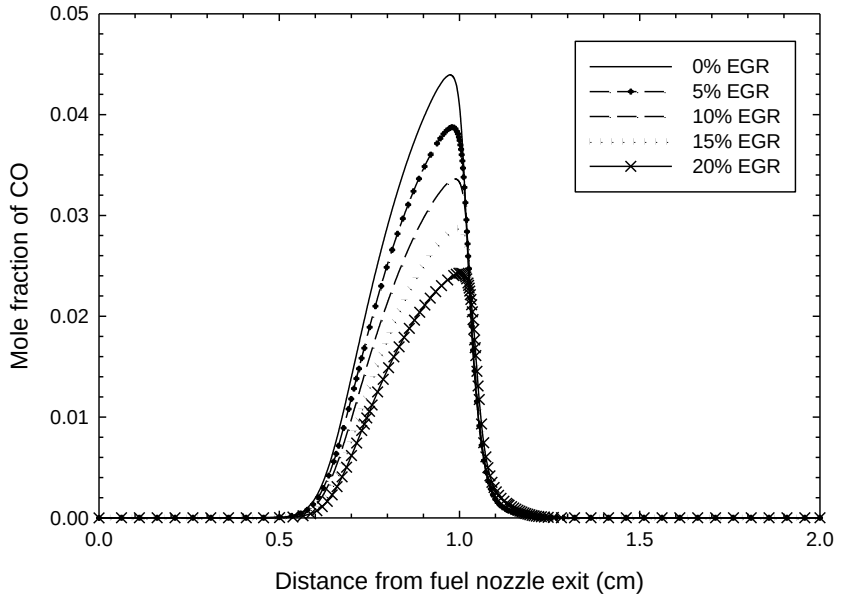

Figure 3-13 Mole fraction of CO vs. axial co-ordinate for different amounts of EGR.

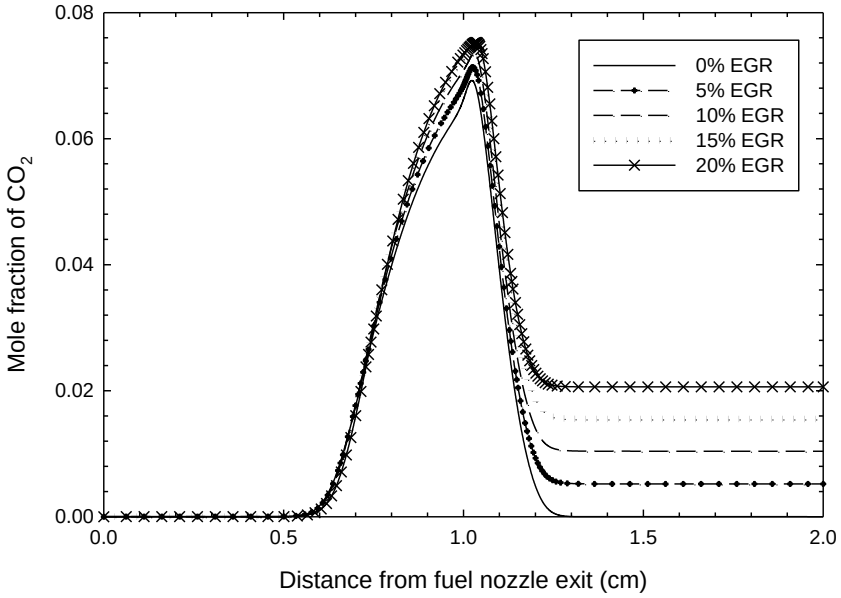

Figure 3-14 Mole fraction of CO_2 vs. axial co-ordinate for different amounts of EGR.

Figures 3-12shows mole fraction of H_2O plotted against distance from the fuel nozzle exit. The H_2O profiles for all EGR fractions are seen to have nearly identical peak values and peak locations. The difference in H_2O mole fractions at the oxidizer end are due to increase caused by introduction of EGR into the oxidizer stream.

Peak CO mole fractions are significantly affected by introduction of EGR, as seen from fig. 3-13. The effects of EGR on the rate of the CO_2 formation reaction ($CO + H_2O \rightarrow CO_2 + H_2$) are significant. At higher EGR fractions, CO is rapidly consumed to produce CO_2. This is seen as a reduction in peak CO mole fractions. The location of the peak also moves towards oxidizer side. Since mole fraction of methane fuel is one for all cases but the fraction of combustible oxygen reduces with increasing EGR, the reacting species become richer in fuel. Hence the flame stabilizes closer to the oxidizer exit.

Figure 3-14 shows variation in CO_2 mole fraction with distance from the fuel nozzle exit. The peak CO_2 mole fraction increases slightly with increase in EGR fraction. However, the location of the peak is nearly the same for all cases.

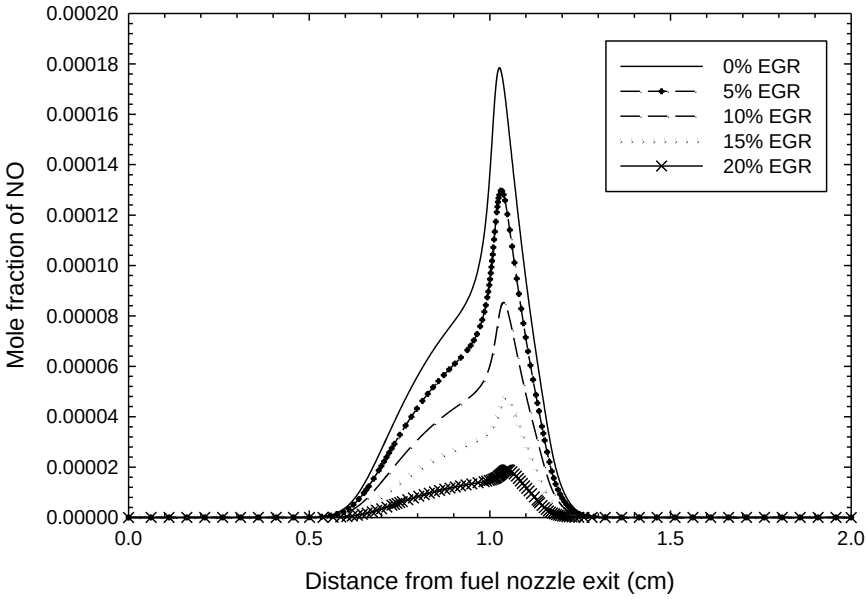

Figure 3-15 Mole fraction of NO vs. axial co-ordinate for different amounts of EGR.

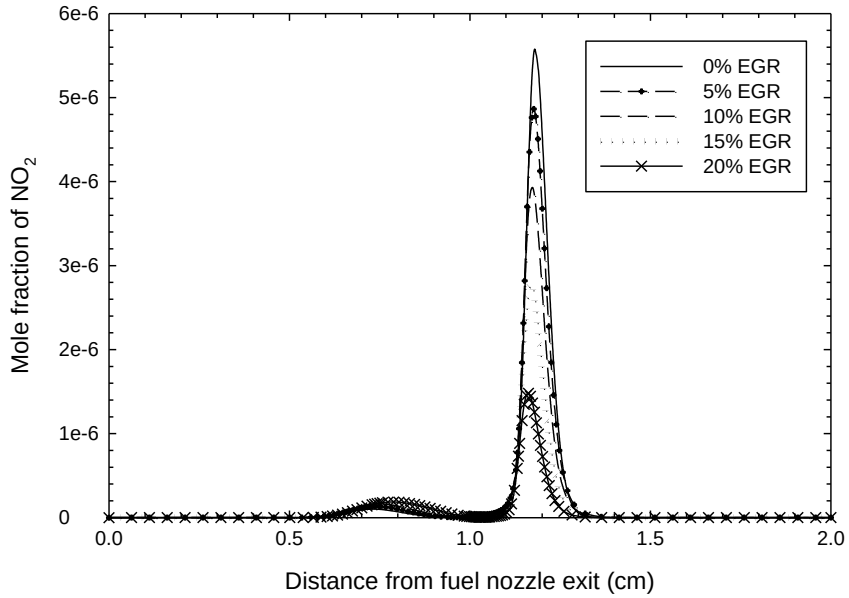

Figure 3-16 Mole fraction of NO_2 vs. axial co-ordinate for different amounts of EGR.

Figures 3-15 and 3-16 show variation in NO and NO_2 mole fractions with distance from fuel nozzle exit, for different values of EGR percentage. It is observed that the peak NO mole fraction reduces by an order of magnitude with change in EGR fraction from 5% to 25%. This can be directly correlated to lower peak flame temperatures, since the initiation step for the thermal mechanism ($N_2 + 0 \rightarrow NO + N$)is highly temperature sensitive.

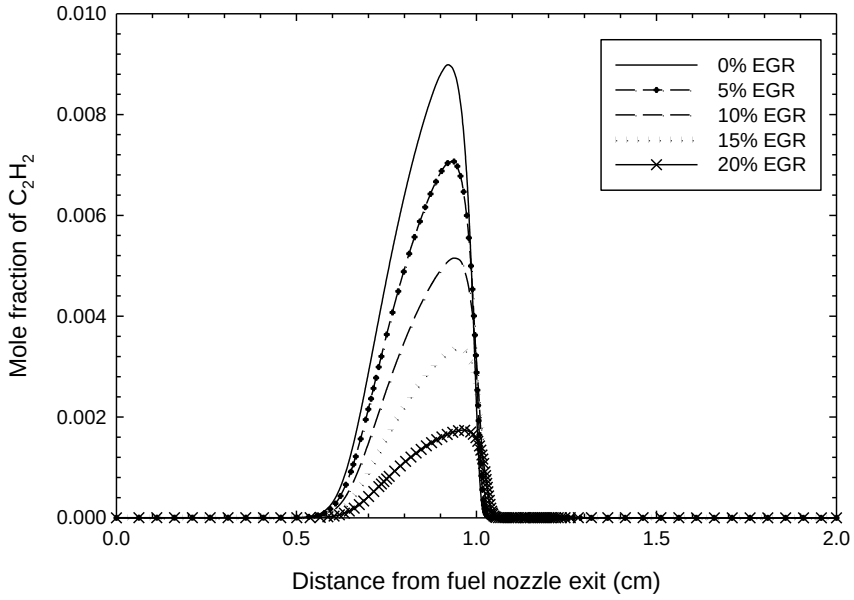

Figure 3-17 Mole fraction of C_2H_2 vs. axial co-ordinate for different amounts of EGR.

Figure 3-17 shows mole fraction of C_2H_2 peaking at the same location where the smaller NO2 mole fraction peak is seen in fig. 3-16. Both these species are part of the NO formation mechanism.

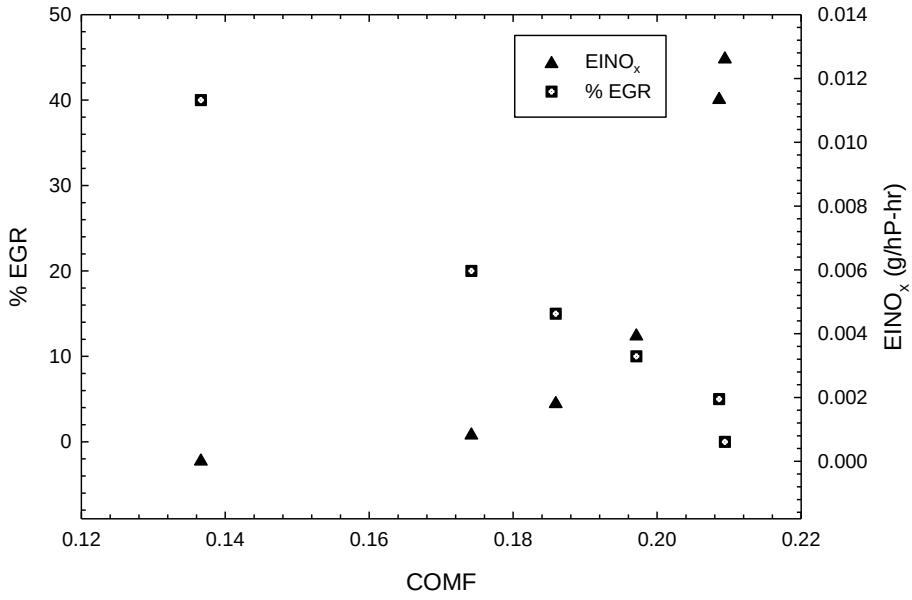

Figure 3-18 $EINO_x$ vs. COMF for EGR variation at constant pressure and inlet temperature (1 bar, 300 K) with OPPDIF.

Figure 3-18 shows both the % EGR (Left Y axis) and the emission index of NO_x (Right Y axis) plotted against the combustible oxygen mass fraction. As expected, with increase in EGR fraction, the value of COMF diminishes. COMF is inversely related to the amount of EGR introduced in the reacting species. This is due to the fact that the exhaust gas, containing carbon dioxide and water vapor as the major species, displaces oxygen from the incoming fresh air stream (Agarwal et al. 2011). The lower oxygen fraction contributes to lowering the total amount of NO_x generated. In addition, the exhaust gas species have higher specific heat and therefore act as a heat sink, causing the peak reaction temperature to lower (Adi et al. 2009; Abd-Alla 2002).

3.3 Effect of Variation in Preheat

In Diesel engines with typical compression ratio between 18 and 20, the temperature of in-cylinder air at the end of compression stroke is of the order of 1000 K. The condition at the end of compression can be simulated by considering preheated oxidizer and fuel creating the diffusion flame. To analyze the effect of preheat on the structure and NO_x emissions of counterflow methane-air diffusion flames, three different flames were simulated. Only inlet temperature for both - fuel and oxidizer was changed. The pressure was maintained at 1 bar, EGR fraction was constant at 15%, and strain rate was specified to be 20 s^{-1} for all simulations.

The following figures show the effect of preheat on the structure and NOx emissions of the flames under study. The computed wet based mole fractions are presented below.

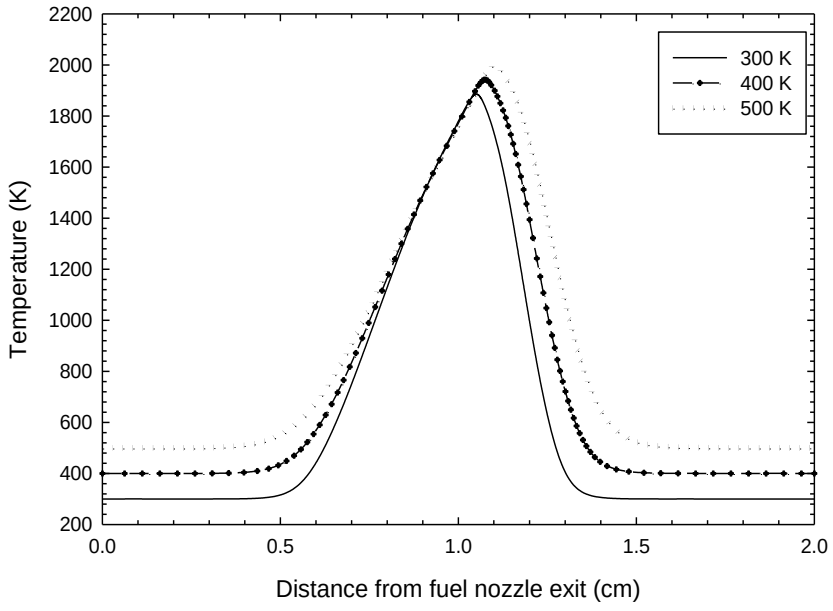

Figure 3-19 Temperature vs. axial co-ordinate for effect of preheat.

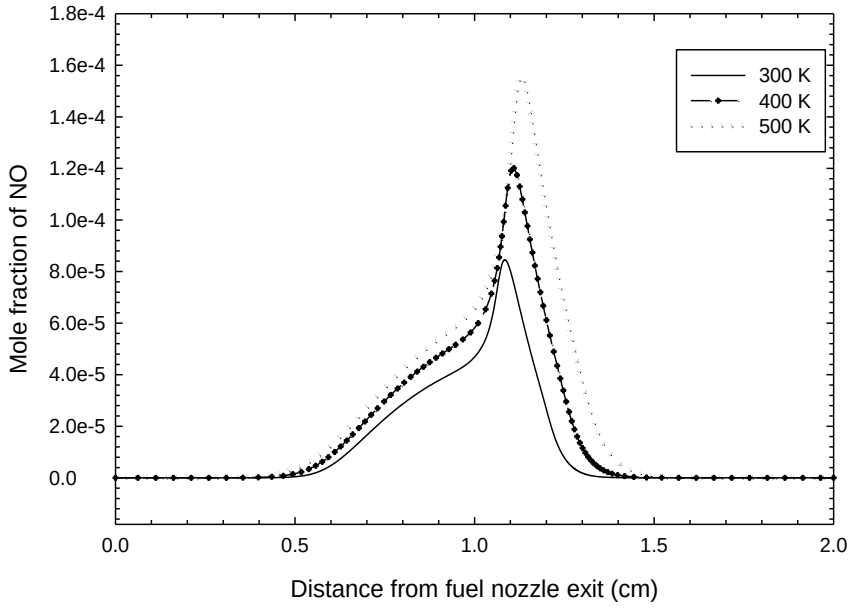

Figure 3-20 Mole fraction of NO vs. axial co-ordinate for effect of preheat.

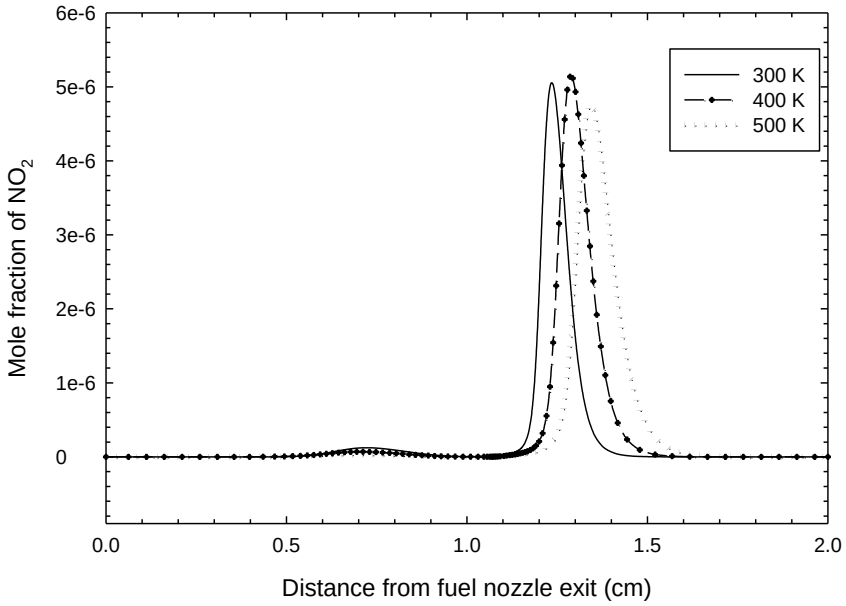

Figure 3-21 Mole fraction of NO_2 vs. axial co-ordinate for effect of preheat.

Figure 3-19 shows variation of temperature with distance from the fuel nozzle exit for various degrees of preheat. With increment in the initial temperature of fuel and

oxidizer, the peak flame temperature increases and location of peak flame temperature moves towards the oxidizer stream with increasing preheat. This affects production of NO_x, as can be seen from figures 3-20 and 3-21. The increase in NO mole fraction with preheat is more pronounced than that in NO_2 mole fraction. The increased rates of the initiation reaction of the prompt mechanism are responsible for the increase in the NO mole fractions with preheat. The rates of the thermal mechanism also increase significantly, but for the present conditions, the NO concentrations are still dominated by the prompt route (Lim et al. 2000)

3.4 Effect of variation in Pressure

In typical naturally aspirated Diesel engines, the in-cylinder air pressure at the end of compression is around 40 bar. To analyze the effect of pressure on the structure and NO_x emissions of counterflow methane-air diffusion flames, three different flames were simulated with pressure being the only varied parameter. The fuel and oxidizer inlet temperature was maintained at 300 K, EGR fraction at 15%, and strain rate was specified to be 20 s^{-1} for all simulations. The computed wet based mole fractions are presented below.

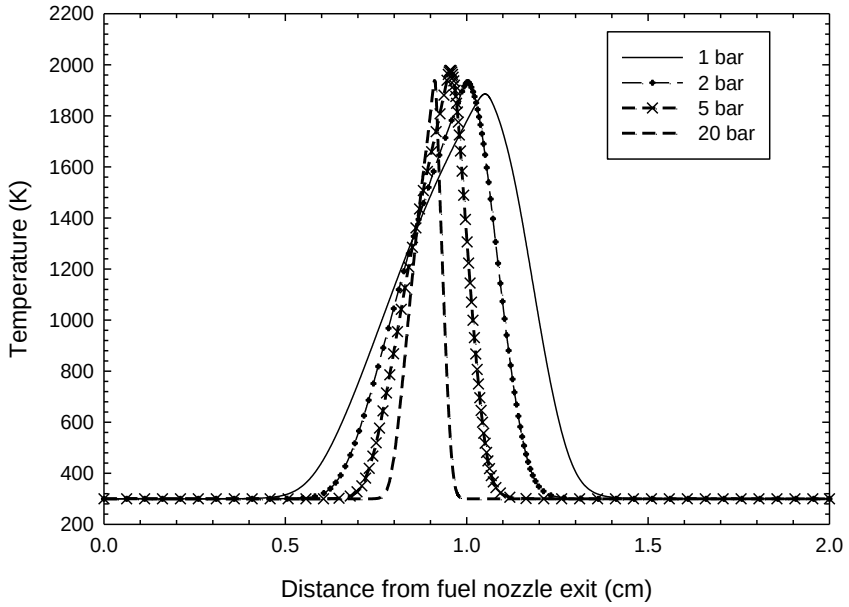

Figure 3-22 Temperature vs. Distance from fuel nozzle exit for different pressures.

Figure 3-22 shows temperature variation with distance from the fuel nozzle exit for various operating pressures. With increasing pressure, the peak flame temperature increases and the location of peak flame temperature moves towards richer mixture fractions with increasing pressure. This affects NO_x proportions in the flames, as can be seen from fig.3-23 and 3-24.

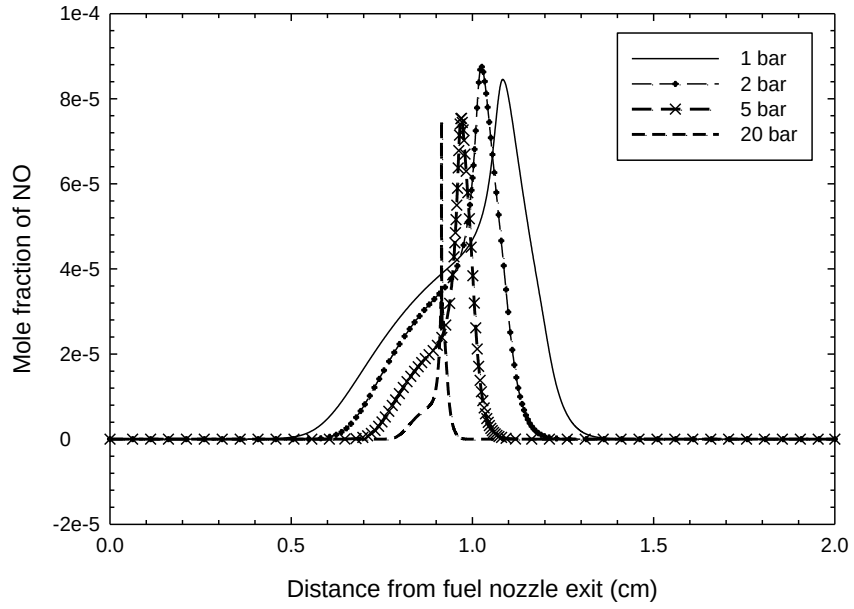

Figure 3-23 Mole fraction of NO vs. axial co-ordinate for different pressures.

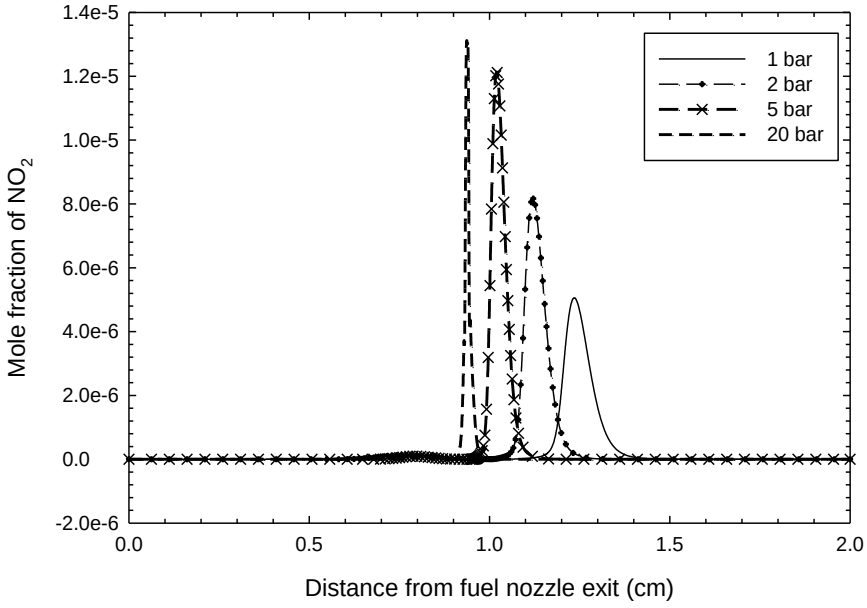

Figure 3-24 Mole fraction of NO_2 vs. axial co-ordinate for different pressures.

As seen from fig. 3-23, the peak NO mole concentration initially increases with rising pressure and then decreases as the pressure continues increasing as observed experimentally using LIF previously (Naik 2004). Previous studies on high pressure flames have shown existence of a similar behavior in temperature and NO_x emissions with pressure variation up to 3 MPa (Figura and Gomez, 2012). Reaction zones narrow with increasing pressure, as observed from fig. 3-22 to 3-24. The effect of pressure on NOx emissions is significant but when normalized by the heat release rate which also increases with pressure, the $EINO_x$ shows less sensitivity.

3.5 Effect of Variation in Strain rate

In a Diesel flame inside a compression ignition engine, strain rate can vary between 10000 s^{-1} near the fuel injector to 10 s^{-1} farthest from the injector (Akinyemi 1997). To analyze the effect of strain rate on the structure and NO_x emissions of counterflow methane-air diffusion flames, three different flames were simulated. Strain rate was varied between 20 s^{-1} and 40 s^{-1}. The fuel and oxidizer inlet temperature was maintained at 300 K, EGR fraction at 15%, and pressure at 1 bar for all simulations. Low strain rate flames are affected more by radiation, than high strain rate flames. Since radiation is a critical parameter for temperature and therefore, NO_x, such flames are important for the present study. The computed wet based mole fractions are presented below.

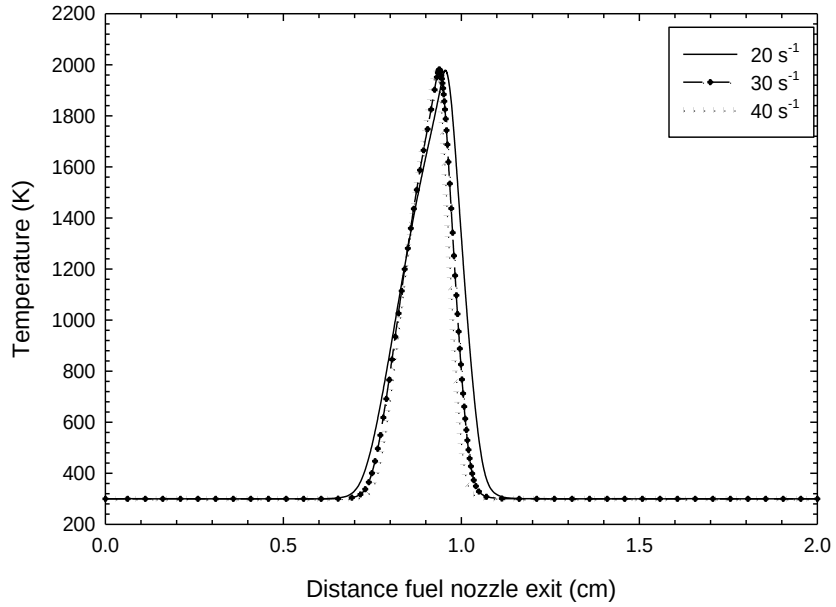

Figure 3-25 Temperature vs. axial co-ordinate for effect of strain rate.

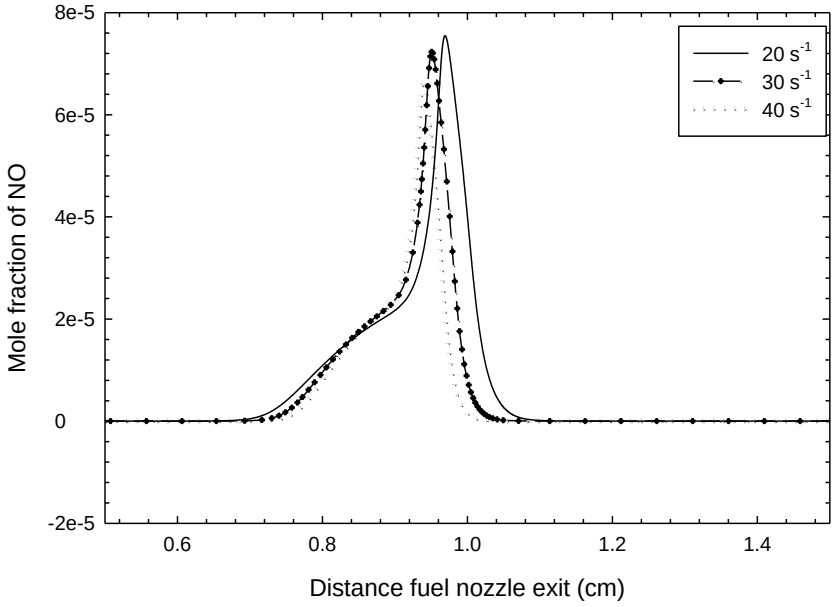

Figure 3-26 Mole fraction of NO vs. axial co-ordinate for effect of strain rate.

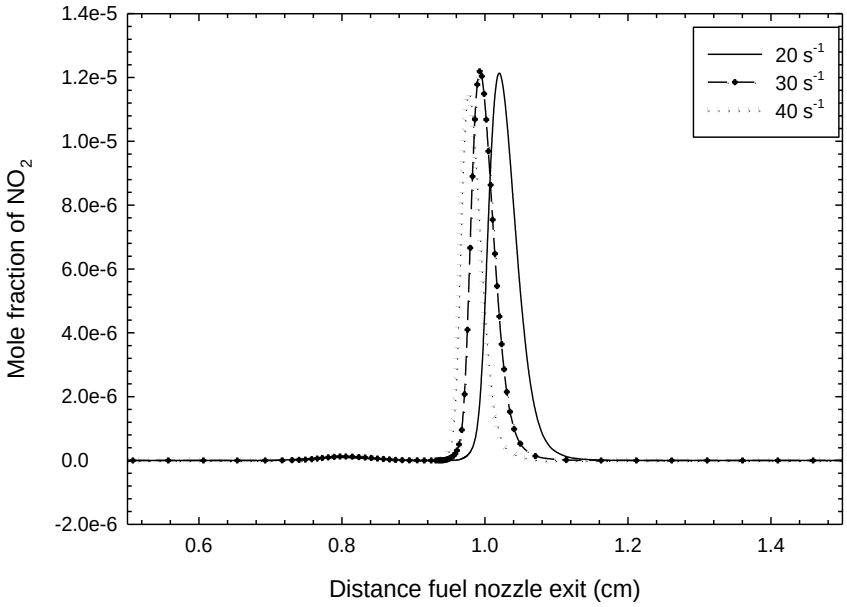

Figure 3-27 Mole fraction of NO_2 vs. axial co-ordinate for effect of strain rate.

Figure 3-25 shows temperature variation with distance from the fuel nozzle exit for various strain rate values. It is observed that the current range of strain rates does not have a significant effect on the temperature profile of the flames. The peak flame temperature as well as location of the peak is not affected with alteration in strain rate. However, NO and NO_2 mole fractions along the nozzle axis show changes with variation in strain rate. Flames with higher strain rate are seen to have lower peak NO and NO_2 mole fractions. Also, the NO_x peak moves toward the fuel stream with increasing strain rate.

CHAPTER 4. CONCLUSIONS AND RECOMMENDATIONS FOR FUTURE WORK

4.1 Effect of Exhaust Gas Fraction

The contribution of exhaust gas recirculation in lowering NO_x emissions of methane-air counterflow diffusion flames is demonstrated through figure 4-1. In Diesel engines, exhaust gases lower the oxygen concentration inside the cylinder and increase the specific heat of the intake air mixture, which results in lower flame temperatures. The present flame simulation study supports the theory that reduced availability of oxygen and lower flame temperatures affect NO and NO_2 formation and destruction reactions.

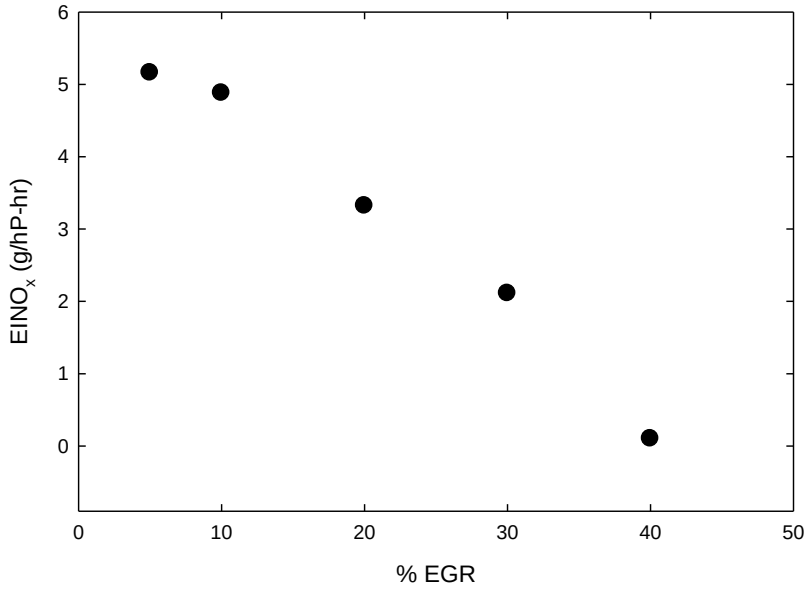

Figure 4-1 $EINO_x$ vs. EGR for 20 bar, 1000 K counterflow diffusion flame.

4.2 Effect of pressure and preheat

The effect of pressure and preheat on EINOx for counterflow diffusion flames is illustrated in fig.4-2. The global strain rate for these simulations is constant at 20 s^{-1}.

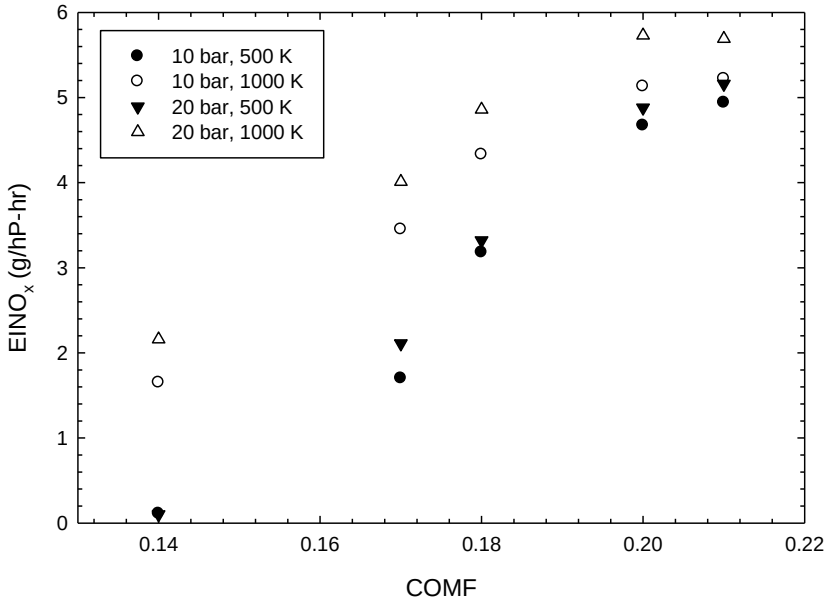

Figure 4-2 EINOx vs. COMF with variation in preheat and pressure.

Figures 4-2 shows that with increase in preheat, emission index of NO_x rises significantly. The same behavior is observed with increase in pressure. However, the effect of increment in pressure is more pronounced at lower pressures and flattens out at higher pressures. Thus, the present study shows that the EINOx – COMF relationship for methane/air diffusion flames at pressure and temperature conditions emulating CI engine conditions is similar to that seen in CI engine experiments.

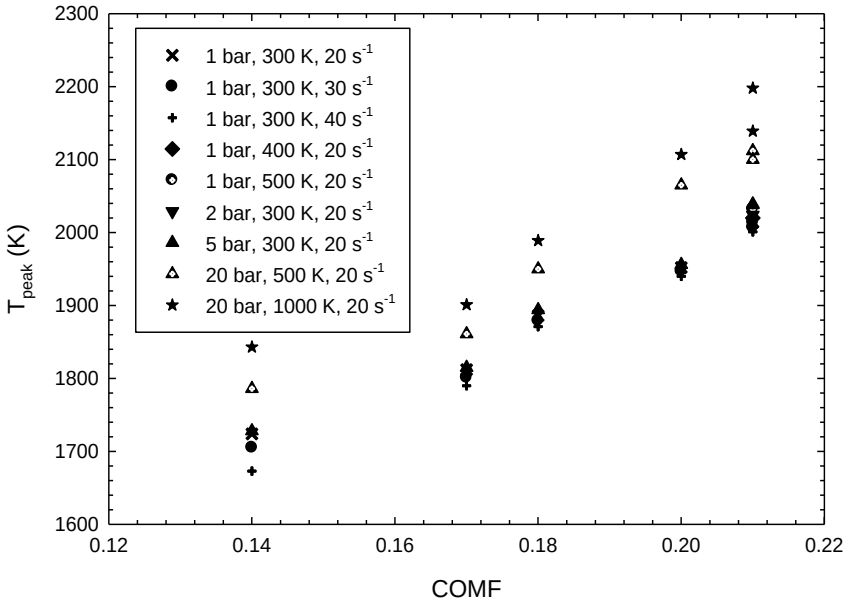

Figure 4-3 Peak flame temperature vs. percentage of EGR.

Figure 4-3 shows variation in the peak flame temperature with COMF. Pressure and preheat being constant, flames with lower strain rates are seen to have higher peak flame temperatures. The expected direct relations between pressure and flame temperature, as well as, preheat and flame temperature, are observed.

4.3 Comparison of Engine data with Flame Computations

Figure 4-4 compares engine experimental results (Adi 2012) related to NO_x emission index with the present flame computations for studying the effect of exhaust gas recirculation. The experimental data was derived from tests on a 6.7 L Diesel engine with a compression ratio of 17.3, which correspond to a pressure of 40 bar and temperature of about 1000 K at the end of compression.

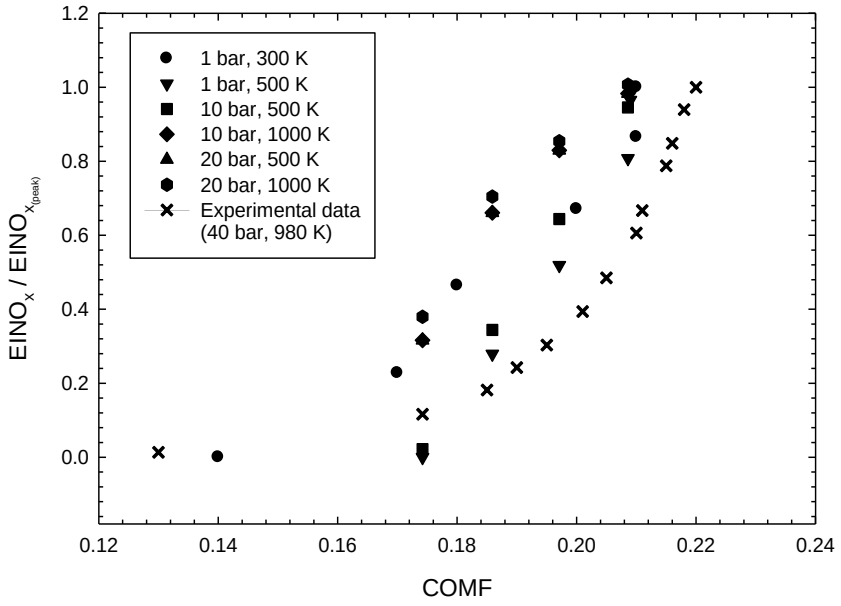

Figure 4-4 Experimental and computational normalized EINOx vs. COMF.

Although the working fluid for the engine experiments and flame computations is not alike, it is observed that the $EINO_x$ – COMF relationship holds in both cases. Increase in NOx emissions with increase in COMF is observed in Diesel engines as well as methane-air diffusion flame calculations.

4.4 Quantitative Reaction Pathway Analysis

In order to understand how the GRI mechanism models NO formation via the prompt pathway(Douglas 1999), it is informative to look at Quantitative Reaction Path Diagrams (QRPDs) associated with flames from this study. Figures 4-5 to 4-7 illustrate the effect of EGR on QRPDs for the flames under consideration. In a QRPD, the net specific rate at which a particular reaction is occurring is calculated at each grid point using a Chemkin post processing package (Kee et al. 1996). These rates are then numerically integrated along the central axis of the flame to obtain a total net specific reaction rate throughout the flame and the integrated rates are then scaled to a maximum value. Those reactions with integrated rates above a threshold percentage (20% for the current study) are shown graphically on a reaction path diagram. The thickness of the arrow representing each reaction is chosen to be proportional to its integrated net specific reaction rate. In this case, a 2 point thickness of the arrow corresponds to a scaled reaction rate of 20% of maximum reaction rate. In cases where multiple reactions proceed between two molecules, such multiple reactions were typically combined into one arrow for the sake of simplicity and clarity. For the current work, only nitrogen kinetics were considered.

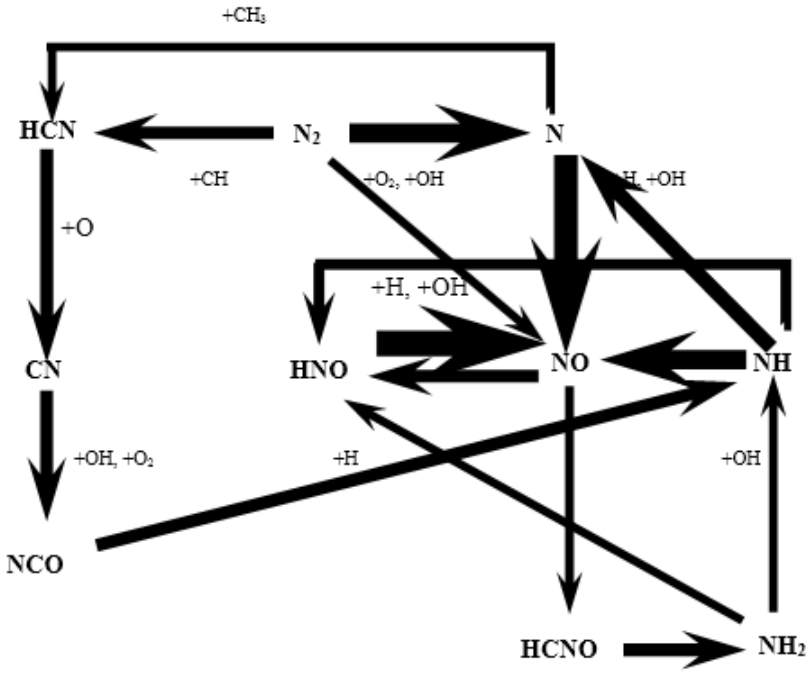

Figure 4-5 QRPD at 1 bar, 300 K, no EGR.

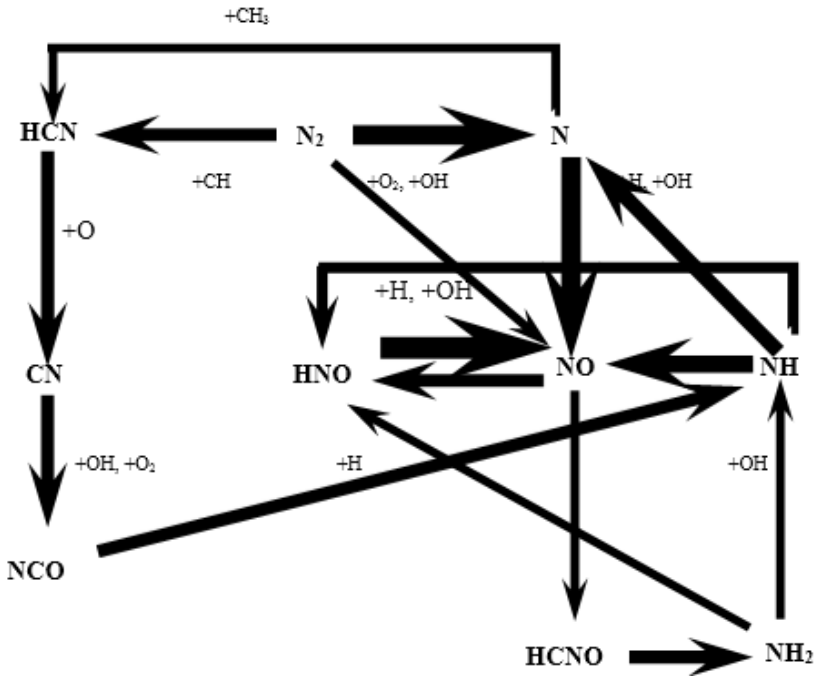

Figure 4-6 QRPD at 1 bar, 300 K, 10% EGR.

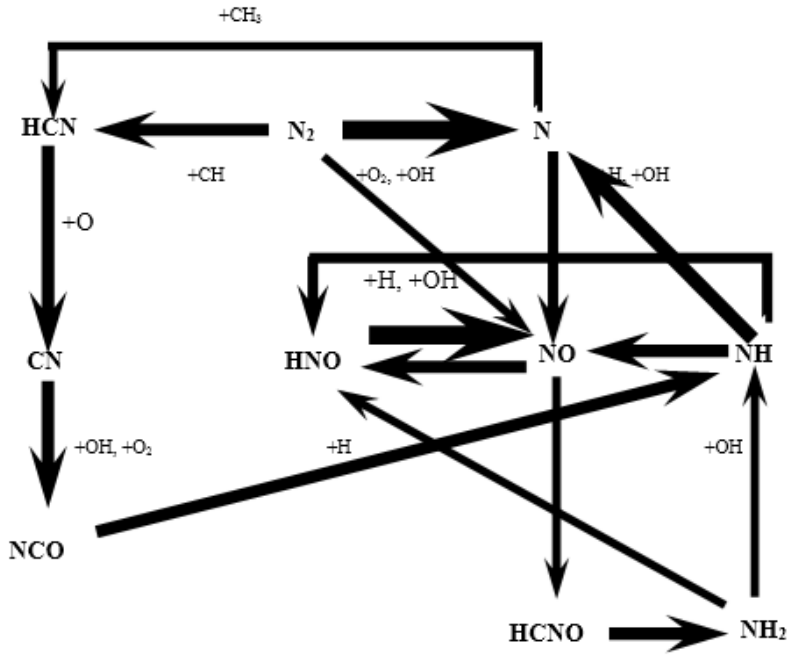

Figure 4-7 QRPD at 1 bar, 300 K, 20% EGR.

In the combustion of fuels that contain no nitrogen, nitric oxide is formed by four chemical mechanisms or routes that involve nitrogen from the air: the thermal or Zeldovich mechanism, the Fenimore or prompt mechanism, the N_2O-intermediate mechanism and the NNH mechanism. The thermal mechanism dominates in the high temperature region, whereas the Fenimore mechanism is more important in rich combustion.

The thermal or Zeldovich mechanism consists of two chain reactions given by

$$O + N_2 \leftrightarrow NO + N. \tag{19}$$

$$k_{17,f} = 1.8 \cdot 10^{11} exp[-38370/T(K)]. \tag{20}$$

and $$N + O_2 \leftrightarrow NO + O. \tag{21}$$

$$k_{19,f} = 1.8 \cdot 10^{11} exp[-4680/T(K)]. \tag{22}$$

The activation energy for eq. (19) is given in eq. (20).It has a very strong temperature dependence. Introduction of EGR leads to lower peak flame temperatures as seen in section 3-2. The lower peak flame temperatures affect the thermal NO formation pathway. This is represented by the successive thinning of the $N \rightarrow NO$ arrow in figures 4-5 to 4-7.

4.4.1 Combustible Oxygen Mass Fraction and (F/Ox).

Figure 4-8 is a plot of EINOx vs. (F/Ox) for counterflow methane-air diffusion flames with different EGR fractions. With introduction of higher fractions of EGR, the O mole fraction in the oxidizer stream reduces compared to air alone. This leads to an increase in the (F/Ox) ratio represented here. The global stoichiometric mixture fraction is also affected. Figure 4.9 indicates a monotonic reduction in the emission index of NOx with increment in stoichiometric fuel air ratio.

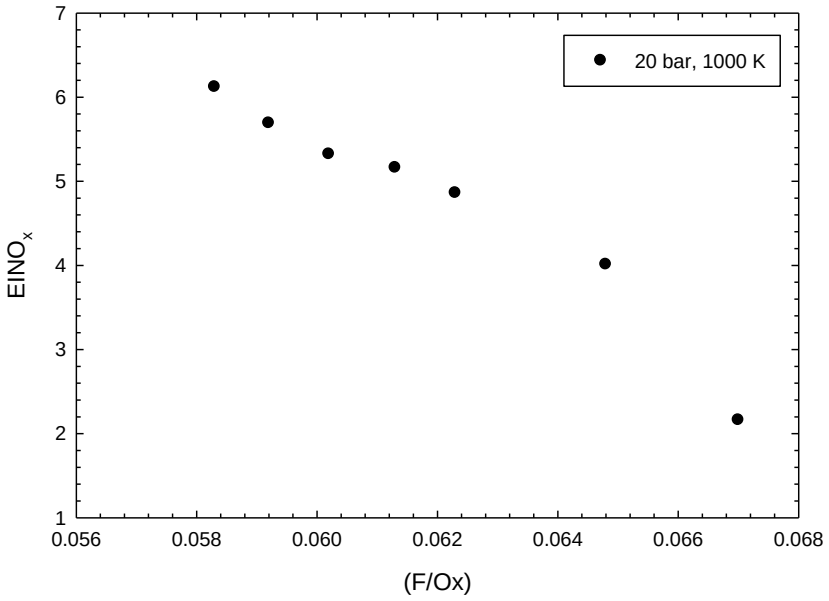

Figure 4-8 EINO$_x$ vs. (F/Ox) for 20 bar, 1000 K.

Figure 4-9 illustrates an almost linear relationship between COMF and stoichiometric fuel-air ratio over most of the range.

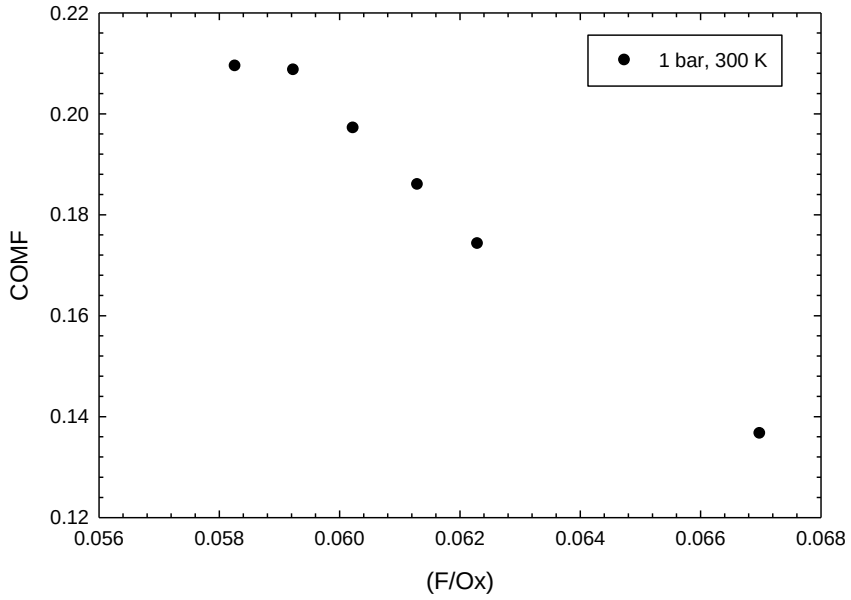

Figure 4-9 COMF vs. (F/Ox).

4.5 Recommendations for Future Work

1. Detailed chemistry calculations with either n-heptane or other Diesel surrogates to mimic Diesel engine situations are essential for validating the $EINO_x$ – COMF relationship observed from engine experiments.
2. Calculations with A/F ratios in the range employed in Diesel engines are required.
3. Studies of premixed and partially premixed flames with EGR. This will help in truly understanding flame behavior inside a Diesel engine cylinder.
4. Study of flames with wider range of strain rates.
5. Experiments with recirculated exhaust gases will help in understanding how EGR affects combustion.
6. Use of mechanisms with better modeling of the prompt NO formation pathway.

LIST OF REFERENCES

LIST OF REFERENCES

Abd-Alla, G.H., 2002. Using exhaust gas recirculation in internal combustion engines: a review. *Energy Conversion and Management*, 43(8), pp.1027–1042.

Adi, G., 2012. PhD Dissertation: Closed Loop Control for Biodiesel Blends in Mixing Controlled Combustion,*Purdue University*.

Adi, G. Hall, Snyder, D., C, Bunce, M, Satkoski, C.,Kumar, S.,Garimella, P., Stanton, D., Shaver, G., 2009. Soy-Biodiesel Impact on NO x Emissions and Fuel Economy for Diffusion-Dominated Combustion in a Turbo−Diesel Engine Incorporating Exhaust Gas Recirculation and Common Rail Fuel Injection. *Energy & Fuels*, 23(12), pp.5821–5829.

Agarwal, D., Singh, S.K. & Agarwal, A.K., 2011. Effect of Exhaust Gas Recirculation (EGR) on performance, emissions, deposits and durability of a constant speed compression ignition engine. *Applied Energy*, 88(8), pp.2900–2907.

Akinyemi, O.C., 1997. PhD Dissertation: A Flame Sheet Model of Combustion and NO Formation in Diesel Engines, *Massachusetts Institute of Technology*.

Berta, P., Aggarwal, S. & Puri, I., 2006. An experimental and numerical investigation of n-heptane/air counterflow partially premixed flames and emission of NOx and PAH species. *Combustion and Flame*, 145(4), pp.740–764

Bilger, R.W., 1988. Proceedings of the Combustion Institute. , p.475.

Bilger, R.W., 2006. Reaction Rates in Diffusion Flames. , pp.277–284.

Blevins, L.G.Renfro, M., Lyle, K., Laurendeau, N., Gore, J., 1999. Experimental study of temperature and CH radical location in partially premixed CH4/air coflow flames. *Combustion and Flame*, 118(4), pp.684–696.

Blevins, L.G., 1996. PhD Dissertation: NOx Emission Characteristics of Gas-fired Radiant Tube Flames : The Role of Partial Premixing. *Purdue University*.

Blevins, L.G. & Gore, J.P., 1999. Computed Structure of Low Strain Rate Partially Premixed CH 4 / Air Counterflow Flames : Implications for NO Formation. *Combustion and Flame*, 566(1), pp.546–566.

Briones, a, Som, S. & Aggarwal, S., 2007. Effect of multistage combustion on NOx emissions in methane–air flames. *Combustion and Flame*, 149(4), pp.448–462.

Chadwick, B.L.,Morrison, R. J. S., Campisi, A., Thomson, D. D., Laurendeau, N. M., 2001. Laser-Induced Fluorescence Measurements and Modeling of Nitric Oxide in Premixed Flames of $CO+H_2+CH_4$ and Air at High Pressures *Combustion and Flame*, 2180(00).

Chandler, J.M. Cannon, W., Neerman, J., 2012. Engine Variables and Their Effects on Exhaust Gas Composition, (March 2012), pp.37–41.

Chen, J.Y., Liu, Y. & Rogg, B., 1993. CO-H2-N2/Air Diffusion Flames: Thermal Radiation and Transient Effects. *Reduced Kinetic Mechanisms for Applications in Combustion Systems*. Springer-Verlag, Berlin-Heidelberg, pp. 196–223.

Dixon-Lewis, G., David, T., Gaskell, P. S., Fukatani, S., Jinno, H., Miller, J., Kee, R., Smooke, M.,Peters, N., Effelsberg, E.,Warnatz, J., Behrendt, F., 1985. Twentieth Symposium (International) on Combustion. *The Combustion Institute*, p.1893.

Douglas, D., 1999. PhD Dissertation: Measurements and Modeling of Nitric Oxide Formation in Counterflow, Premixed, CH4/O2/N2 flames,*Purdue University.*

Figura, L. & Gomez, A., 2012. Laminar counterflow steady diffusion flames under high pressure (P>=3MPa) conditions. *Combustion and Flame*, 159(1), pp.142–150.

Hahn, W.A. & Wendt, J.O.L., 1981. Eighteenth Symposium (International) on Combustion. *The Combustion Institute*, p.121.

Heywood, J., 1988. *Internal Combustion Engine Fundamentals*, New York: Mc.Graw Hill, Inc.

Jangi, M., Lucchini, T., D'Errico, G., Bai, X., 2013. Effects of EGR on the structure and emissions of diesel combustion. *Proceedings of the Combustion Institute*, 34(2), pp.3091–3098.

Kampa, M. & Castanas, E., 2008. Human health effects of air pollution. *Environmental pollution (Barking, Essex : 1987)*, 151(2), pp.362–7.

Kee, R.J., Rupley, F., Meeks, E., Miller, J., 1996. Chemkin Overview.

Lim, J., 1998. PhD Dissertation: A study of the Effects of Preheat and Steam Addition on the Flame Structure and NO Formation in Laminar Counterflow Flames. *Purdue University*.

Lim, J., Gore, J. & Viskanta, R., 2000. A Study of the Effects of Air Preheat on the Structure of Methane / Air Counterflow Diffusion Flames. *Combustion and Flame*, 274, pp.262–274.

Lutz, A.E., Kee, R., Grcar, J.,Ruply, F., 1996. OPPDIF: A Fortran Program for Computing Opposed-flow Diffusion Flames. *Sandia report SAND96-8243*.

Maub, F., Keller, D. & Peters, N., 1990. A Lagrangian Simulation of Flamelet Extinction and Re-ignition in Turbulent Jet Diffusion Flames. , pp.693–698.

Naha, S. & Aggarwal, S.K., 2004. Fuel effects on NOx emissions in partially premixed flames. *Combustion and Flame*, 139(1-2), pp.90–105.

Naik, S. V., 2004. PhD Dissertation:Laser-Induced Fluorescence Measurements and Modeling of Nitric Oxide and Methylidyne in Laminar, Counter-flow Partially Premixed Flames at High Pressure. *Purdue University*.

Paul, K.T., Hull, T.R.,Lebek, K., Stek, A.A., 2008. Fire smoke toxicity: The effect of nitrogen oxides. *Fire Safety Journal*, 43(4), pp.243–251.

Peters, N. & Williams, F.A., 1983. Journal of the American Institute of Aeronautics and Astronautics. *Proceedings of the Combustion Institute*, pp.423–429.

Plee, S.L. (General M.R.L. et al., 1982. Diesel NOx Emissions - A Simple Correlation Technique for Intake Air Effects. *Nineteenth Symposium (Intl.) on Combustion*, pp.1495–1502.

Rotexo Copyright Document, 2010. 1-D and Counterflow Flames.

Schlichting, H., 1968. Boundary Layer Theory,*McGraw-Hill*.

Schneider, C.G. & Hill, L.B., 2005. Diesel and Health in America : The Lingering Threat. , *www.catf.us/goto/dieselhealth.*

Seshadri, K., 2005. Counterflow Extinction of Premixed and Nonpremixed Methanol and Ethanol Flames. *University of California Energy Institute's Energy Policy and Economics Working Paper Series*.

Sivathanu, Y.R. & Faeth, G.M., 1990. Generalized State Relationships for Scalar Properties in Nonpremixed Hydrocarbon / Air Flames. *Combustion and Flame*, 0.

Smith, G.P., Golden, D., Frenklach, M., Moriarty, N., Eiteneer, B.,Golgenberg, M., Bowman, T., Hansen, R., Song, S., Gardiner, W., Lissianski, V., Qin, Z., http://www.me.berkeley.edu/gri_mech/.

Tsuji, H. & Yamaoka, I., 1967. Eleventh Symposium (International) on Combustion. *The Combustion Institute,* pp.979.

Turns, S., 2010. An Introduction to Combustion,*McGraw Hill.*

US Environmental Protection Agency, http://www.epa.gov/region1/eco/diesel/basic_info.html.

Vranos, A. & Hall, R.J., 1993. Influence of Radiative Loss on Nitric Oxide formation in Counterflow Diffusion Flames at High Pressure. *Combustion and Flame,* 238, pp.230–238.

Zhu, X.L. & Gore, J.P., 2005. Radiation Effects on Combustion and Pollutant Emissions of High-pressure Opposed Flow Methane/Air Diffusion Flames. *Combustion and Flame*, 141(1-2), pp.118–130.

APPENDIX

APPENDIX

Study Of Premixed Flames

The aim of the study was to analyze the effects of excess CO_2 on combustion phenomena including NO_x control, stability and CO emissions by considering the effects of the re-circulated CO_2, H_2O, pressure and preheat.

A.1 Effect of Exhaust Gas Recirculation

For the purpose of simulating a premixed flame as seen in gas turbines, a lean premixed fuel/oxidizer/CO_2/H_2O was chosen. For a designed lean premixed equivalence ratio of $\emptyset$ and a designed EGR fraction, x, the reactant mixture on the basis of one mole of natural gas approximated as methane is defined by the equation

$$CH_4 + \left(\frac{2}{\emptyset} - x\left(\frac{2}{\emptyset} - 2\right)\right) O_2 + \frac{7.56}{\emptyset}(1+x)N_2 + xCO_2 + 2xH_2O. \quad (23)$$

Selecting $\emptyset$ =0.7, the following with different amounts of exhaust recirculation were formulated as described in Table A-1:

Table A-1 Reacting species composition for analyzing effect of EGR on premixed flames.

Case	$\emptyset$	x	**CH_4**	**O_2**	**N_2**	**CO_2**	**H_2O**
1	0.7	0	1	2.86	10.74	0	0
2	0.7	0.1	1	2.86	11.82	0.1	0.2
3	0.7	0.2	1	2.86	12.89	0.2	0.4

The flame structure and NO_x emissions with variation in EGR are discussed below.

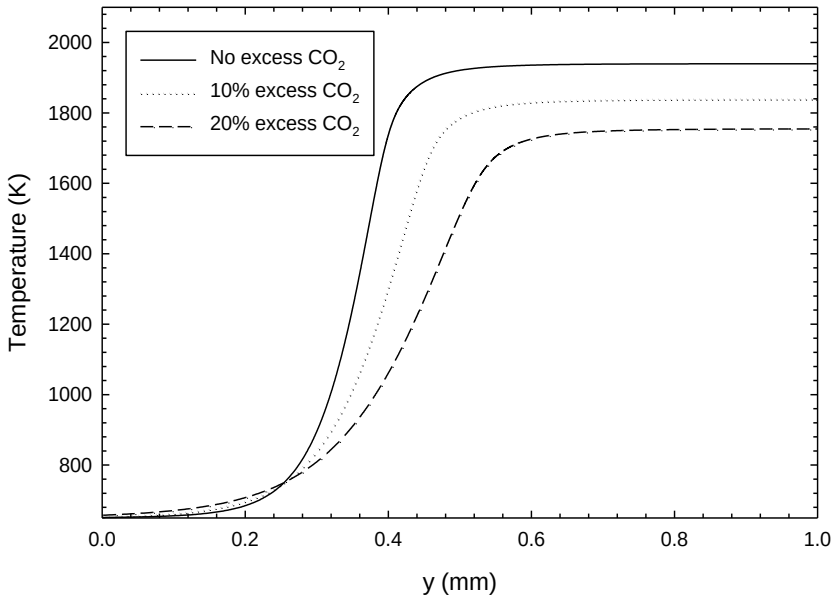

Figure A 1 Temperature vs. distance with variation in CO_2 and H_2O for premixed flames.

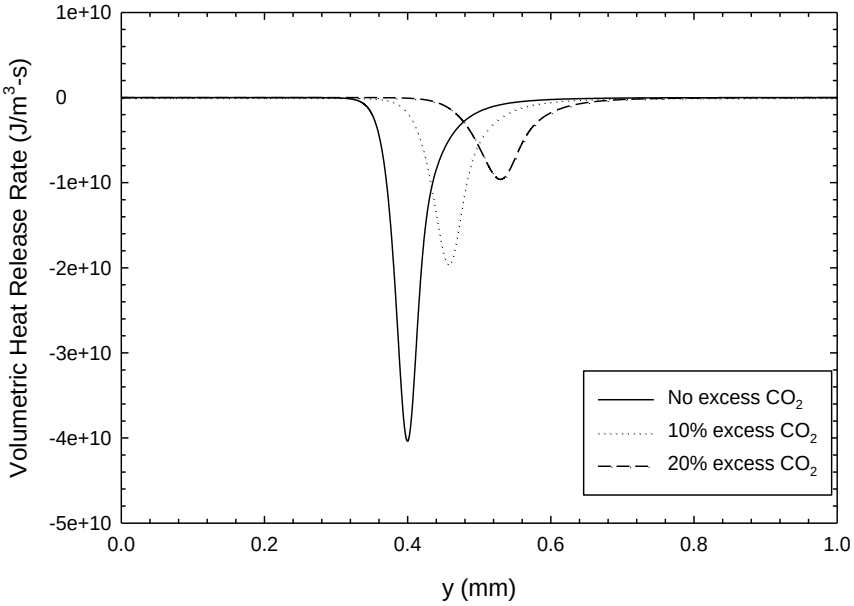

Figure A 2 Volumetric heat release rate vs. distance with variation in CO_2 and H_2O for premixed flames.

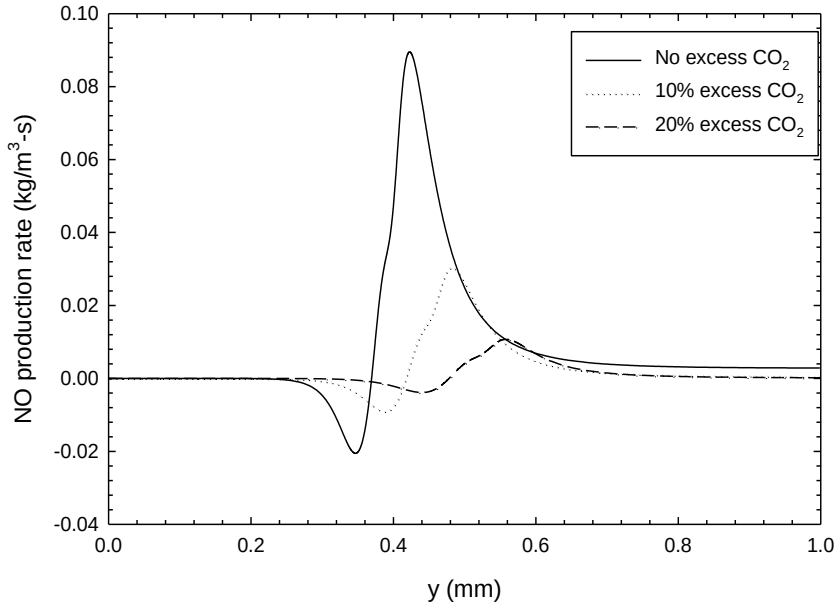

Figure A 3 NO production rate vs. distance with variation in CO_2 and H_2O for premixed flames.

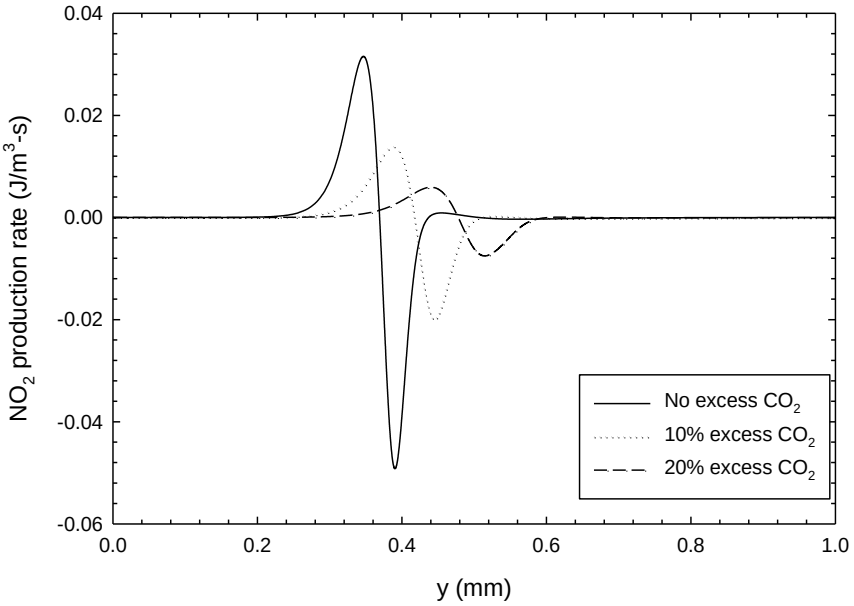

Figure A 4 NO_2 production rate vs. distance with variation in CO_2 and H_2O for premixed flames.

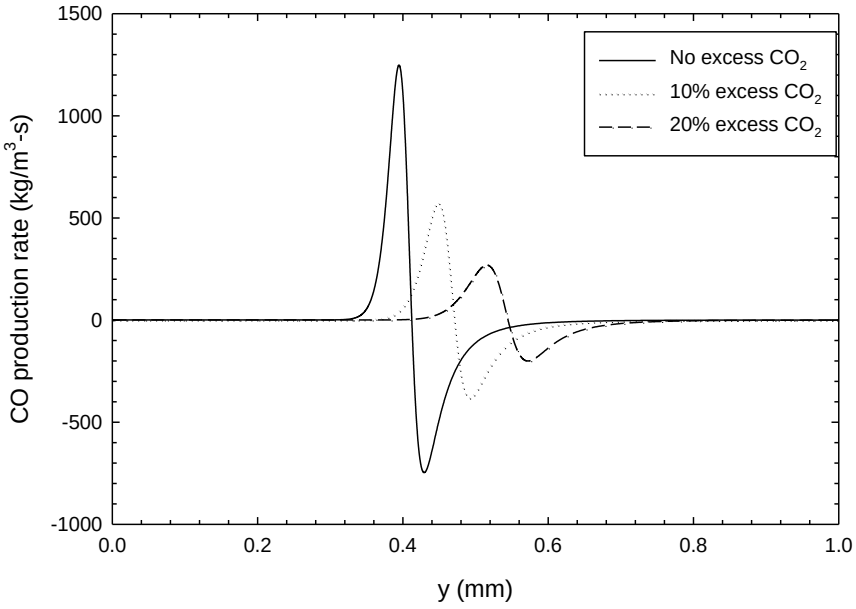

Figure A 5CO production rate vs. distance with variation in CO_2 and H_2O for premixed flames.

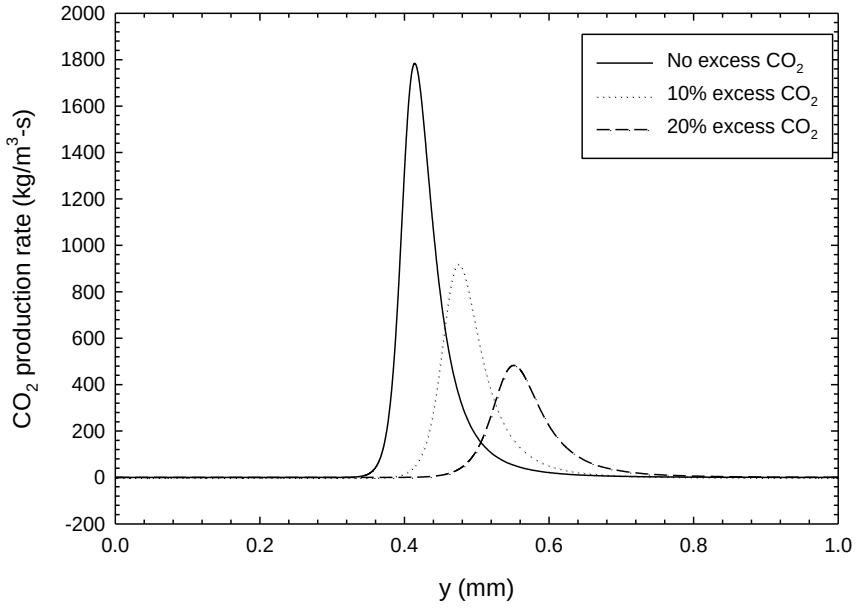

Figure A 6 CO_2 production rate vs. distance with variation in CO_2 and H_2O for premixed flames.

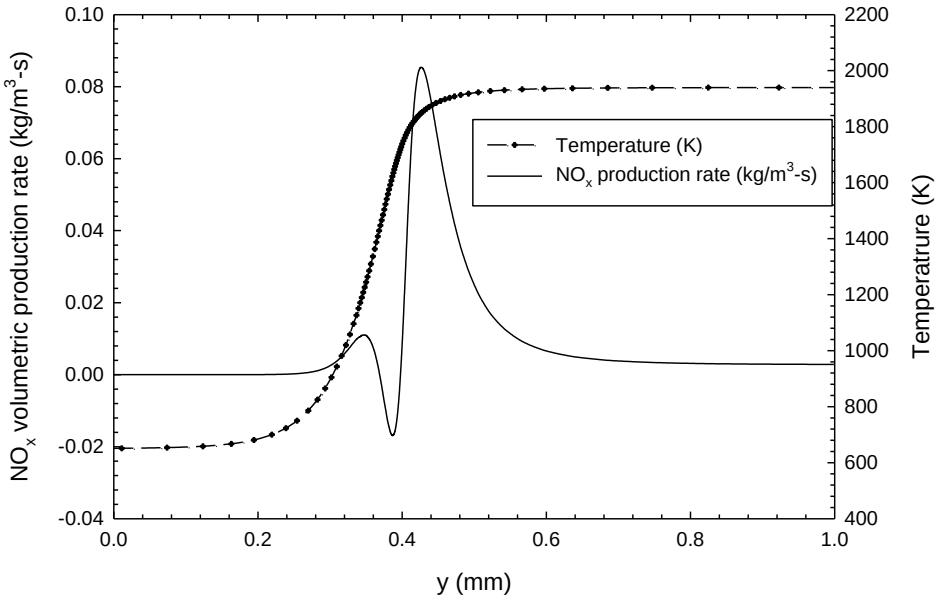

Figure A 7 NO_x production rate and temperature vs. distance for no CO_2 and H_2O addition for premixed flames.

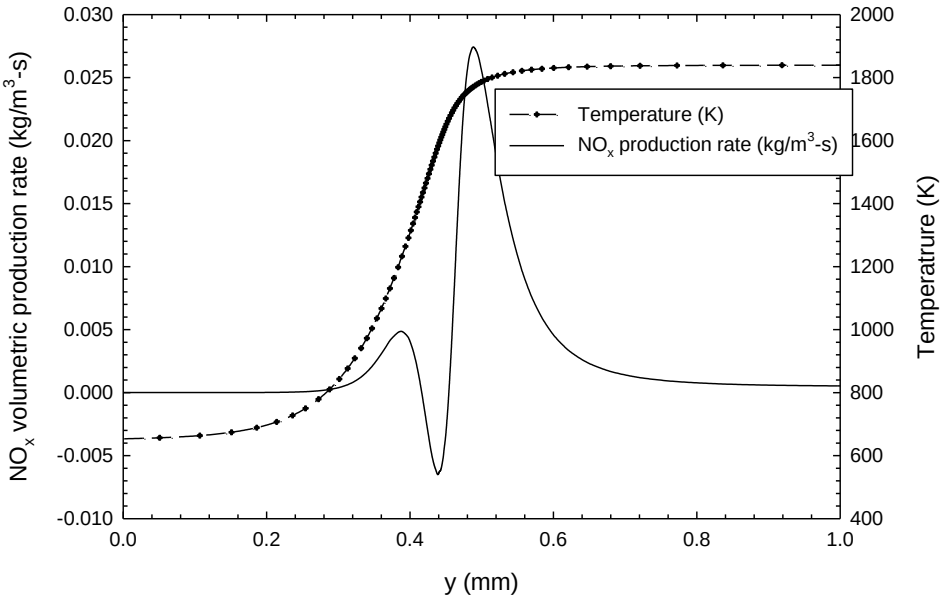

Figure A 8 NO_x production rate and temperature vs. distance for 10% excess CO_2 and H_2O on for premixed flames.

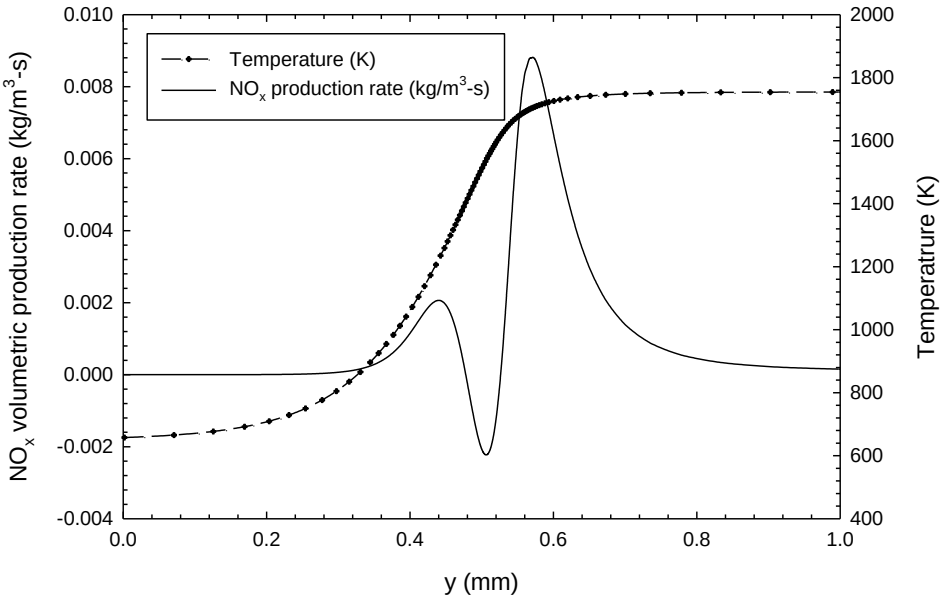

Figure A 9 NOx production rate and temperature vs. distance for 20% excess CO_2 and H_2O on for premixed flames.

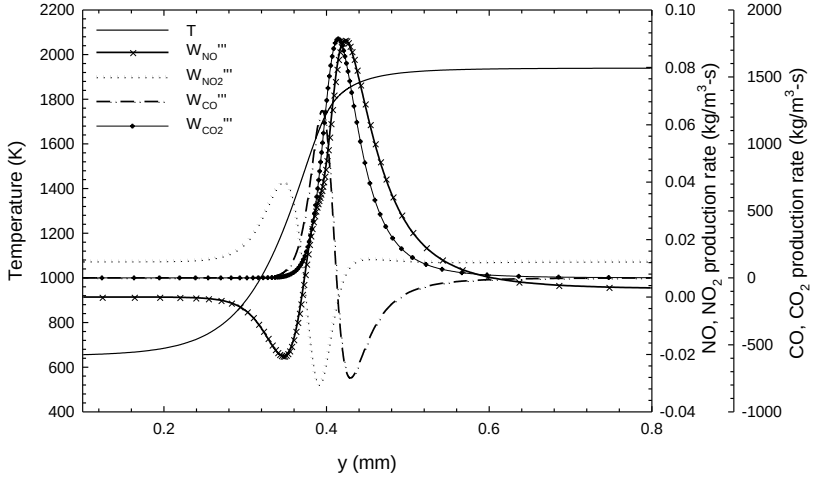

Figure A-10 Flame structure and pollutant production rates for premixed methane/air flame at 10 bar, 650 K, $\Phi = 0.6$, 0 moles of CO_2.

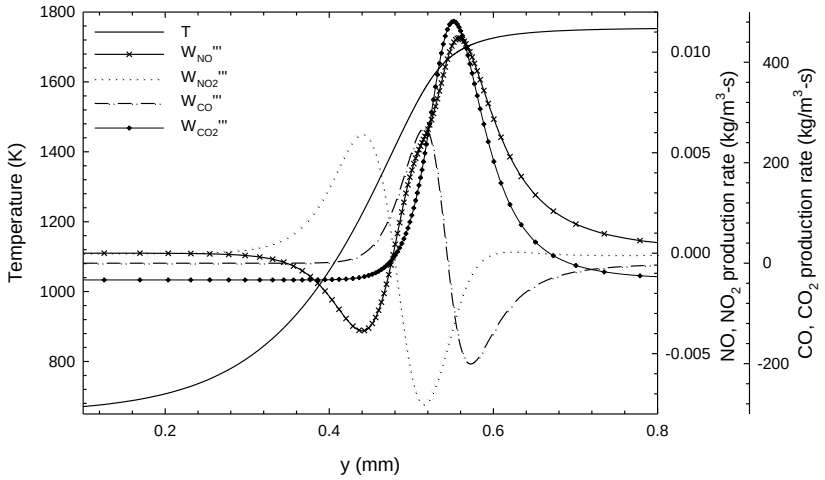

Figure A-11 Flame structure and pollutant production rates for premixed methane/air flame at 10 bar, 650 K, Φ = 0.6, 0.2 moles of CO_2.

A.2 Effect of Preheat

To study the effect of preheat on premixed, two flames with initial reactant temperatures of 650 K and 850 K were considered. The effect of preheat on the structure and emissions of the premixed flames are illustrated in the following figures.

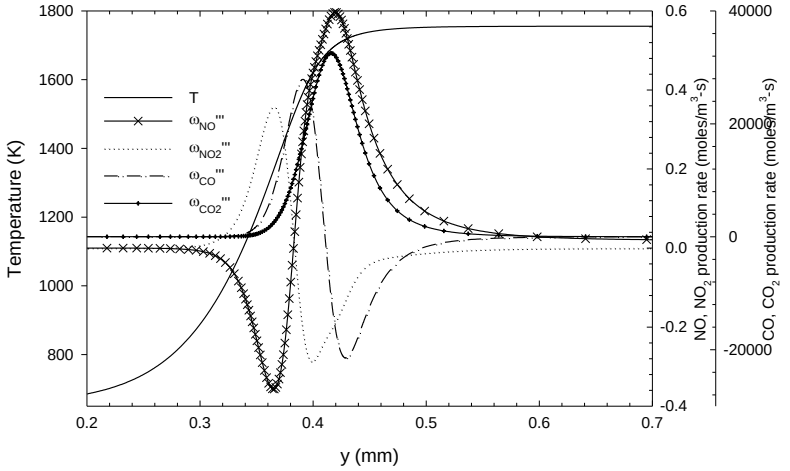

Figure A-12 Flame structure and pollutant production rates for premixed methane/air flame at 30 bar, 650 K, Φ = 0.6, 0.2 moles of CO_2.

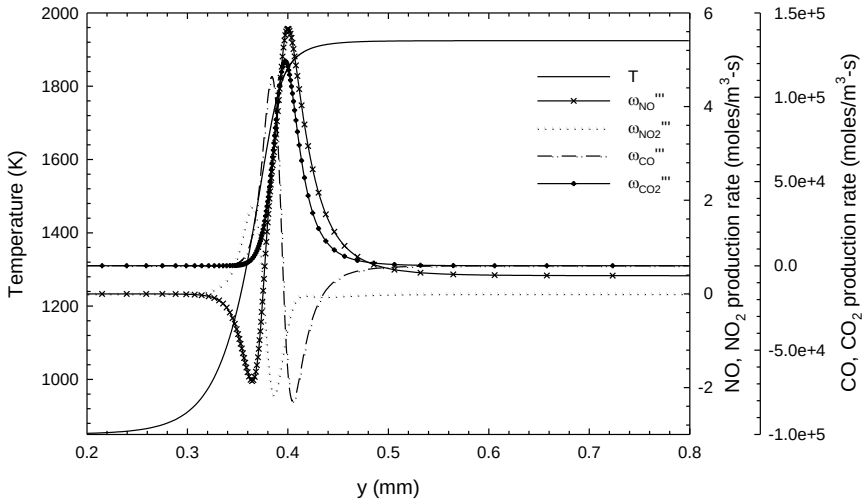

Figure A-13Flame structure and pollutant production rates for premixed methane/air flame at 30 bar, 850 K, $\Phi = 0.6$, 0.2 moles of CO_2.

A.3 Effect of Pressure.

To study the effect of pressure on premixed, two flames at of 10 bar and 30 bar were considered. The effect of pressure on the structure and emissions of the premixed flames are illustrated in the following figures.

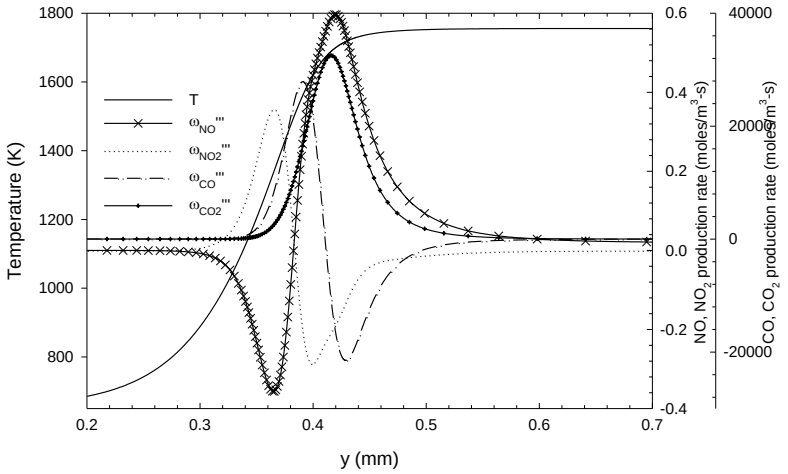

Figure A-14 Flame structure and pollutant production rates for premixed methane/air flame at 10 bar, 650 K, Φ = 0.6, 0.2 moles of CO_2.

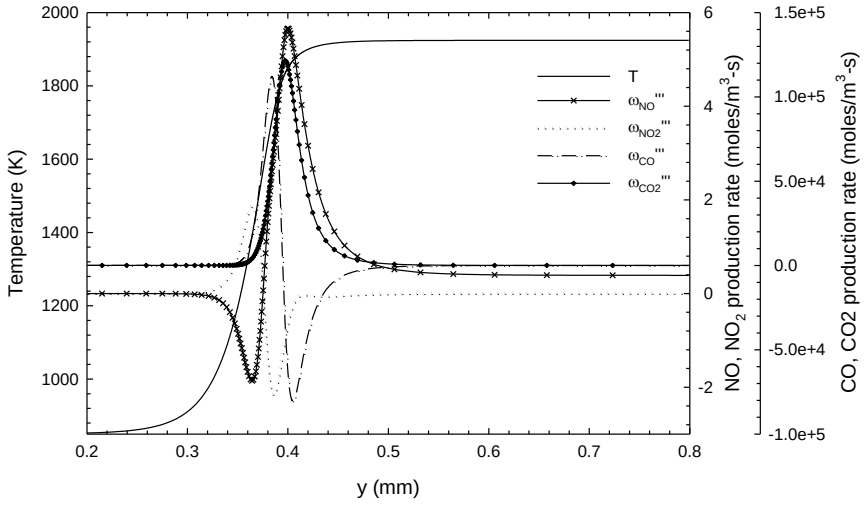

Figure A-15 Flame structure and pollutant production rates for premixed methane/air flame at 30 bar, 650 K, Φ = 0.6, 0.2 moles of CO_2.

Addition of CO_2 and H_2O to the reacting species leads to a decrement in the peak flame temperature for the premixed flames as can be seen from the figures above. The thermal mechanism is the dominant pathway for NO production in premixed flames and therefore, a corresponding drop in NO and NO_2 mass fractions is observed.

VITA

VITA

Mugdha Shriram Sane

Education
B.E., Mechanical Engineering, 2011, Pune University, India
M.S.M.E., 2013, Purdue University, West Lafayette, Indiana

Mugdha is currently working as an engineer at Cummins Inc., Columbus, Indiana.

PUBLICATIONS

PUBLICATIONS

Sane, M., Dasappa, S., Shaver, G., Gore, J., 2013. Effect of Exhaust Gas Recirculation and Combustible Oxygen Mass Fraction on Emission Index of NOx for Counterflow Methane/Air Diffusion Flames, *8th U.S. National Combustion Meeting,* Utah, USA, May 19-22, 2013.